International Journal of Mechanical Sciences 53 (2011) 1050–1068

Contents lists available at SciVerse ScienceDirect

International Journal of Mechanical Sciences

journal homepage: www.elsevier.com/locate/ijmecsci

# Investigation on steady state deformation and free vibration of a rotating inclined Euler beam

Ming Hsu Tsai [a], Wen Yi Lin [b], Yu Chun Zhou [a], Kuo Mo Hsiao [a,*]

[a] Department of Mechanical Engineering, National Chiao Tung University, Hsinchu, Taiwan, ROC
[b] Department of Mechanical Engineering, De Lin Institute of Technology, Tucheng, Taiwan, ROC

ARTICLE INFO

*Article history:*
Received 5 March 2011
Received in revised form
4 June 2011
Accepted 24 August 2011
Available online 31 August 2011

*Keywords:*
Rotating inclined beam
Steady state deformation
Vibration
Natural frequency
Corotational formulation
Finite element method

ABSTRACT

The steady state deformation and infinitesimal free vibration around the steady state deformation of a rotating inclined Euler beam at constant angular velocity are investigated by the corotational finite element method combined with floating frame method. The element nodal forces are derived using the consistent second order linearization of the nonlinear beam theory, the d'Alembert principle and the virtual work principle in a current inertia element coordinates, which is coincident with a rotating element coordinate system constructed at the current configuration of the beam element. The rotating element coordinates rotate about the hub axis at the angular speed of the hub. The equations of motion of the system are defined in terms of an inertia global coordinate system, which is coincident with a rotating global coordinate system rigidly tied to the rotating hub. Numerical examples are studied to demonstrate the accuracy and efficiency of the proposed method and to investigate the steady state deformation and natural frequency of the rotating inclined beam.



## 1. Introduction

Rotating beams are often used as a simple model for propellers, turbine blades, and satellite booms. Rotating beam differs from a non-rotating beam in having additional centrifugal force and the Coriolis effects on its dynamics. The free vibration frequencies of rotating beams have been extensively studied [1–24]. However, the vibration analysis of rotating beam with inclination angle, which is considered in the recent computer cooling fan design on the natural frequencies of rotating beams [20], is rather rare in the literature [9,18,20,21]. In Refs. [20,21], the effect of the steady state axial deformation and the inclination angle on the natural frequencies of the rotating beam was investigated. However, the lateral steady state deformation and its effects on the natural frequencies of the rotating beam were not considered in Refs. [20,21]. It is well known that the spinning elastic bodies sustains a steady state deformation (time-independent deformation) induced by constant rotation [25]. For rotating beams with an inclination angle as shown in Fig. 1, the steady state deformations include axial deformation and lateral deformation. The linear solution of the steady state deformation of rotating inclined beam induced by constant rotation can be easily obtained using mechanics of materials and is given in Appendix A. However, the centrifugal stiffening effect on the steady lateral deformation is significant for slender rotating inclined beam, and the centrifugal force is configuration dependent load; thus the linear solution of the steady state deformation of rotating inclined beam may be not accurate enough. The lagwise bending and axial vibration of rotating inclined beams are coupled due to the Coriolis effects [14,23] and the lateral steady state deformation. The accuracy of the frequencies obtained from linearizing about the steady state deformation is dependent on the accuracy of the steady state deformation and the accuracy of the linearized perturbation [6,11]. Thus, the geometrical nonlinearities that arise due to steady state deformation should be considered. However, to the authors' knowledge, the lateral steady state deformation and its effects on the lagwise bending and axial vibration of rotating inclined beams are not reported in the literature. The objective of this paper is to investigate the steady state deformation and its effects on the lagwise bending and axial vibration of rotating inclined beams with zero setting angle at constant angular velocity. Here, the large displacement and large rotation, but small strains are considered for the steady state deformation. The equations of motion for a rotating inclined Euler beam at constant angular velocity are derived using a corotational finite element formulation combined with the rotating frame method. The nodal coordinates, displacements and rotations, absolute velocities, absolute accelerations and the equations of motion of the system are defined in terms of an inertia global coordinate system, which is coincident with a rotating global

* Corresponding author.
*E-mail address:* kmhsiao@mail.nctu.edu.tw (K.M. Hsiao).

0020-7403/$ - see front matter © 2011 Elsevier Ltd. All rights reserved.
doi:10.1016/j.ijmecsci.2011.08.011

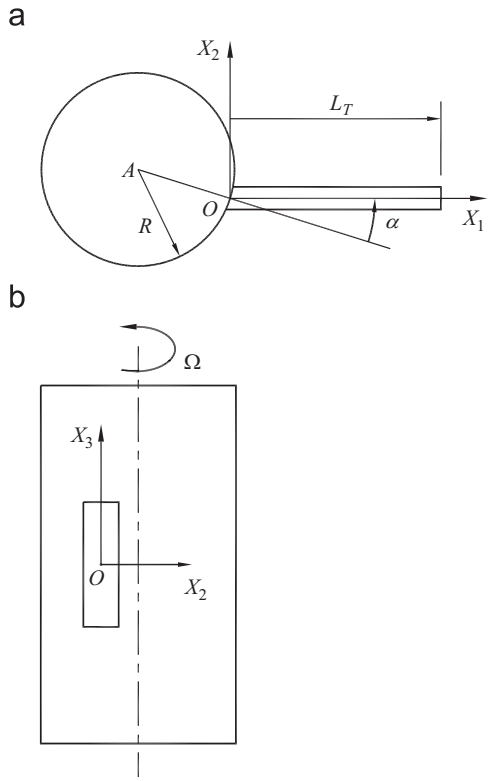


**Fig. 1.** A rotating inclined beam, (a) top view and (b) side view.

coordinate system rigidly tied to the rotating hub, while the total deformations in the beam element are measured in an inertia element coordinate system, which is coincident with a rotating element coordinate system constructed at the current configuration of the beam element. The rotating element coordinates rotate about the hub axis at the angular speed of the hub. The inertia nodal forces and deformation nodal forces of the beam element are systematically derived by the virtual work principle, the d'Alembert principle and consistent linearization of the fully geometrically nonlinear beam theory [26–28] in the element coordinates. The element equations are constructed first in the inertia element coordinate system and then transformed to the inertia global coordinate system using standard procedure. The dominant factors in the geometrical nonlinearities of beam structures are attributable to finite rotations, the strains remaining small. For a beam structure discretized by finite elements, this implies that the motion of the individual elements to a large extent will consist of rigid-body motion. If the rigid-body motion part is eliminated from the total displacements and the element size is properly chosen, the deformation part of the motion is always small relative to the local element axes; thus, in conjunction with the corotational formulation, the higher-order terms of nodal parameters in the element deformation nodal forces and inertia nodal forces may be neglected by the consistent linearization. Due to the consideration of the exact kinematics of the Euler beam, some coupling terms of axial and flexural deformations are retained in the element internal nodal forces.

The infinitesimal free vibrations of rotating beam are measured from the position of the corresponding steady state deformation. The governing equations for linear vibration of rotating beam are obtained by the first order Taylor series expansion of the equation of motion at the position of steady state deformation.

## 2. Formulation

### 2.1. Description of problem

Consider an inclined uniform Euler beam of length $L_T$ rigidly mounted with an inclination angle $\alpha$ on the periphery of rigid hub with radius $R$ rotating about its axis fixed in space at a constant angular speed $\Omega$ as shown in Fig. 1. The axis of the rotating hub is perpendicular to one of the principal directions of the cross section of the beam. The deformation displacements of the beam are defined in an inertia rectangular Cartesian coordinates, which is coincident with a rotating rectangular Cartesian coordinate system rigidly tied to the hub.

Here only axial and lagwise bending vibrations are considered. It is well known that the beam sustains a steady state deformations (time-independent deformation displacements) induced by constant rotation [25]. In this study, large displacement and rotation with small strain are considered in the steady state deformation. The vibration (time-dependent deformation displacements) of the beam is measured from the position of the steady state deformation, and only infinitesimal free vibration is considered. Note that the axial and lagwise vibrations, which are coupled due to the Coriolis effects and the lateral steady state deformation, cannot be analyzed independently. Here the engineering strain and stress are used for the measure of the strain and stress.

### 2.2. Basic assumptions

The following assumptions are made in derivation of the beam element behavior.

(1) The beam is prismatic and slender, and the Euler–Bernoulli hypothesis is valid.
(2) The unit extension of the centroid axis of the beam element is uniform.
(3) The deformation displacements and rotations of the beam element are small.
(4) The strains of the beam element are small.

In conjunction with the corotational formulation, the third assumption can always be satisfied if the element size is properly chosen.

### 2.3. Coordinate systems

In this paper, a corotational formulation combined with the rotating frame method is adopted. In order to describe the system, we define three sets of right handed rectangular Cartesian coordinate systems:

(1) A rotating global set of coordinates, $X_i$ ($i$=1, 2, 3) (see Figs. 1 and 2); the coordinates rotate about the hub axis at a

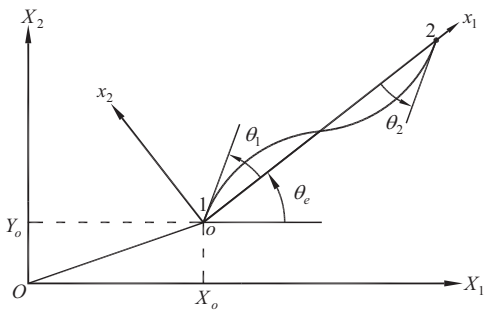


**Fig. 2.** Coordinate systems.

constant angular speed $\Omega$ as shown in Fig. 1. The origin of this coordinate system is chosen to be the intersection of the centroid axes of the hub and the undeformed beam. The $X_1$ axis are chosen to coincide with the centroid axis of the undeformed beam, and the $X_2$ and $X_3$ axes are chosen to be the principal directions of the cross section of the beam at the undeformed state. The direction of the axis of the rotating hub is parallel to the $X_3$ axis. The nodal coordinates, nodal deformation displacements, absolute nodal velocity, absolute nodal acceleration and equations of motion of the system are defined in terms of an inertia global coordinate system, which is coincident with the rotating global coordinate system.

(2) Element coordinates; $x_i$ ($i=1, 2, 3$) (see Fig. 2), a set of element coordinates is associated with each element, which is constructed at the current configuration of the beam element. The coordinates rotate about the hub axis at a constant angular speed $\Omega$. The origin of this coordinate system is located at the element node 1, the centroid of the end section. The $x_1$ axis is chosen to pass through two end nodes of the element; the directions of the $x_2$ and $x_3$ axes are chosen to coincide with the principal direction of the cross section in the undeformed state. Because only the displacements in $X_1X_2$ plane are considered, the directions of $x_3$ axis and $X_3$ axis are coincident. The position vector, deformations, absolute velocity, absolute acceleration, internal nodal forces, stiffness matrices and inertia matrices of the elements are defined in terms of an inertia element coordinate system, which is coincident with the rotating element coordinate system.

In this study, the direction of the axis of the rotating hub is parallel to the $X_3$ axis and only the displacements in $X_1X_2$ plane are considered. Thus, the angular velocity of the hub referred to the global coordinates may be given by

$$\mathbf{\Omega}_G = \{0, \quad 0, \quad \Omega\} \tag{1}$$

where the symbol { } denotes a column matrix, which is used throughout the paper.

### 2.4. Kinematics of beam element

Let $Q$ (Fig. 3) be an arbitrary point in the beam element, and $P$ be the point corresponding to $Q$ on the centroid axis. The position vector of point $Q$ in the undeformed and deformed configurations

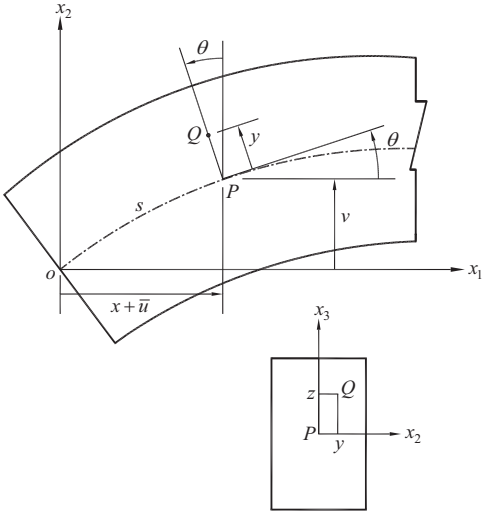


**Fig. 3.** Kinematics of Euler beam.

may be expressed as

$$\mathbf{r}_0 = \{x, y, z\} \tag{2}$$

and

$$\mathbf{r} = \{r_1, r_2, r_3\} = \{x_p(x,t) - y\sin\theta,\ v(x,t) + y\cos\theta,\ z\} \tag{3}$$

$$\sin\theta = \frac{\partial v(x,t)}{\partial s} = \frac{\partial v(x,t)}{\partial x}\frac{\partial x}{\partial s} = \frac{v'}{1+\varepsilon_c} \tag{4}$$

$$\varepsilon_c = \frac{\partial s}{\partial x} - 1 \tag{5}$$

where $x_p(x,t)$ and $v(x,t)$ are the $x_1$ and $x_2$ coordinates of point $P$, respectively, in the deformed configuration, $t$ is time, $\theta=\theta(x,t)$ is the angle counterclockwise measured from $x_1$ axis to the tangent of the centroid axis of the deformed beam, $\varepsilon_c$ is the unit extension of the centroid axis and $s$ is the arc length of the deformed centroid axis measured from node 1 to point $P$. In this paper, $(\,)'$ denotes $(\,)_{,x} = \partial(\,)/\partial x$, $\sin\theta$ is approximated by $\theta$, but the difference between $\theta$ and $v'$ is considered.

Here, the lateral deflection of the centroid axis, $v(x,t)$ is assumed to be the Hermitian polynomials of $x$ and may be expressed by

$$v(x,t) = \{N_1,N_2,N_3,N_4\}^t\{v_1,v_1',v_2,v_2'\} = \mathbf{N}_b^t\mathbf{u}_b \tag{6}$$

where $v_j = v_j(t)$ and $v_j' = v_j'(t)$ ($j=1, 2$) are nodal values of $v$ and $v_{,x}$, respectively, at nodes $j$. Note that, due to the definition of the element coordinates, the values of $v_j$ ($j=1, 2$) are zero. However, their variations and time derivatives are not zero. $N_i$ ($i=1$–$4$) are shape functions and are given by

$$N_1 = \frac{1}{4}(1-\xi)^2(2+\xi), \quad N_2 = \frac{L}{8}(1-\xi^2)(1-\xi)$$
$$N_1 = \frac{1}{4}(1+\xi)^2(2-\xi) \quad N_2 = \frac{L}{8}(-1+\xi^2)(1+\xi) \tag{7}$$

$$\xi = -1 + \frac{2x}{L} \tag{8}$$

where $L$ is the length of the undeformed beam element.

The relationship between $x_p(x,t)$, $v(x,t)$ and $x$ in Eq. (3) may be given as

$$x_p(x,t) = u_1 + \int_0^x [(1+\varepsilon_c)^2 - v_{,x}^2]^{1/2}dx \tag{9}$$

where $u_1$ is the displacement of node 1 in the $x_1$ direction. Note that due to the definition of the element coordinate system, the value of $u_1$ is equal to zero. However, the variation and time derivatives of $u_1$ are not zero.

The axial displacements of the centroid axis may be determined from the lateral deflections and the unit extension of the centroid axis using Eq. (9).

Making use of Eq. (9) and assumptions $v_{,x} \ll 1$ and $\varepsilon_c \ll 1$, one may obtain

$$\ell = L + u_2 - u_1 = x_c(L,t) - x_c(0,t) = \int_0^L \left(1 + \varepsilon_c - \frac{1}{2}v_{,x}^2\right)dx \tag{10}$$

in which $\ell$ is the current chord length of the centroid axis of the beam element, and $u_2$ is the displacement of node 2 in the $x_1$ direction. From Eqs. (6) and (10), $\varepsilon_c$ may be expressed by

$$\varepsilon_c = \frac{1}{L}\left(\mathbf{G}_a^t\mathbf{u}_a + \frac{1}{2}\mathbf{G}_b^t\mathbf{u}_b\right) \tag{11}$$

$$\mathbf{G}_a = \{-1,\ 1\} \tag{12}$$

$$\mathbf{u}_a = \{u_1, u_2\} \tag{13}$$

$$\mathbf{G}_b = \int_0^L \mathbf{N}_b' v_{,x}\, dx \tag{14}$$

where $\mathbf{u}_b$ is defined in Eq. (6).

Substituting Eqs. (9), (11)–(14) into Eq. (3), using the approximation $\cos\theta \approx 1-\frac{1}{2}\theta^2$, $\sin\theta \approx \theta$ and $1/(1+\varepsilon_c) \approx (1-\varepsilon_c)$, retaining all terms up to the second order, the position vector in Eq. (3) may be approximated by

$$\mathbf{r} = \{r_1, r_2, r_3\} = \left\{ x_p - y\theta,\ y\left(1-\frac{1}{2}\theta^2\right)+v,\ z \right\} \tag{15}$$

$$x_p(x,t) = \mathbf{N}_a^t \mathbf{u}_a + x + \frac{x}{2L}\mathbf{G}_b^t \mathbf{u}_b - \frac{1}{2}\int_0^x v_{,x}^2\, dx \tag{16}$$

$$\theta = (1-\varepsilon_c)v' \tag{17}$$

$$\mathbf{N}_a = \left\{ \frac{1-\xi}{2}, \frac{1+\xi}{2} \right\} \tag{18}$$

From Eq. (3) and the definition of engineering strain [29,30], making use of the assumption of small strain, and retaining the terms up to the second order of deformation parameters, the engineering strain in the Euler beam may be approximated by

$$\varepsilon_{11} = \varepsilon_c - (1-\varepsilon_c) y v_{,xx} \tag{19}$$

The absolute velocity and acceleration vectors of point $Q$ in the rotating beam element may be expressed as

$$\mathbf{v} = \{v_1, v_2, v_3\} = \mathbf{v}_o + \boldsymbol{\Omega} \times \mathbf{r} + \dot{\mathbf{r}} \tag{20}$$

$$\mathbf{a} = \{a_1, a_2, a_3\} = \mathbf{a}_o + \dot{\boldsymbol{\Omega}} \times \mathbf{r} + \boldsymbol{\Omega} \times (\boldsymbol{\Omega} \times \mathbf{r}) + 2\boldsymbol{\Omega} \times \dot{\mathbf{r}} + \ddot{\mathbf{r}} \tag{21}$$

$$\mathbf{v}_o = \boldsymbol{\Omega} \times \mathbf{r}_{Ao} \tag{22}$$

$$\mathbf{a}_o = \{a_{o1}, a_{o2}, a_{o3}\} = \boldsymbol{\Omega} \times (\boldsymbol{\Omega} \times \mathbf{r}_{Ao}) \tag{23}$$

$$\boldsymbol{\Omega} = \mathbf{A}_{GE}^t \boldsymbol{\Omega}_G \tag{24}$$

$$\mathbf{r}_{Ao} = \mathbf{A}_{GE}^t \mathbf{r}_{AoG} \tag{25}$$

$$\mathbf{r}_{AoG} = \mathbf{r}_{AO} + \mathbf{r}_{OoG} = \{R\cos\alpha + X_o, -R\sin\alpha + Y_o,\ 0\} \tag{26}$$

where $\mathbf{r}$ is the position point of point $Q$ given in Eq. (15), the symbol $(\dot{})$ denotes time derivative, $\boldsymbol{\Omega}$ is the vector of angular velocity referred to the current inertia element coordinates, $\boldsymbol{\Omega}_G$ is the angular velocity of the hub referred to the global coordinates given in Eq. (1), $\mathbf{A}_{GE}$ is the transformation matrix between the current global coordinates and the current element coordinates, $\mathbf{v}_o$ and $\mathbf{a}_o$ is the absolute velocity and absolute acceleration of point $o$, the origin of the element coordinates, $X_o$ and $Y_o$ are coordinates of point $o$ referred to the current global coordinates, $R$ is the radius of the hub, and $\alpha$ is inclination angle of the rotating beam. $\dot{\mathbf{r}}$ and $\ddot{\mathbf{r}}$ are the velocity and acceleration of point $Q$ relative to the current moving element coordinates. From Eqs. (11)–(18), $\dot{\mathbf{r}}$ and $\ddot{\mathbf{r}}$ may be expressed as

$$\dot{\mathbf{r}} = \{\dot{r}_1, \dot{r}_2, \dot{r}_3\} = \{\dot{x}_p - y\dot{\theta}, \dot{v} - y\dot{\theta}\,\theta, 0\} \tag{27}$$

$$\ddot{\mathbf{r}} = \{\ddot{r}_1, \ddot{r}_2, \ddot{r}_3\} = \{\ddot{x}_p - y\ddot{\theta}, \ddot{v} - y\dot{\theta}^2 - y\ddot{\theta}\theta, 0\} \tag{28}$$

$$\dot{x}_p = \mathbf{N}_a^t \dot{\mathbf{u}}_a + \frac{x}{L}\mathbf{G}_b^t \dot{\mathbf{u}}_b - \int_0^x v_{,x}\dot{v}_{,x}\, dx \tag{29}$$

$$\dot{\theta} = (1-\varepsilon_c)\dot{v}_{,x} - \dot{\varepsilon}_c v_{,x} \tag{30}$$

$$\dot{\varepsilon}_c = \frac{1}{L}(\mathbf{G}_a^t \dot{\mathbf{u}}_a + \mathbf{G}_b^t \dot{\mathbf{u}}_b) \tag{31}$$

$$\ddot{x}_p = \mathbf{N}_a^t \ddot{\mathbf{u}}_a + \frac{x}{L}(\mathbf{G}_b^t \ddot{\mathbf{u}}_b + \dot{\mathbf{G}}_b^t \dot{\mathbf{u}}_b) - \int_0^x (v_{,x}\ddot{v}_{,x} + \dot{v}_{,x}\dot{v}_{,x})dx \tag{32}$$

$$\ddot{\theta} = (1-\varepsilon_c)\ddot{v}_{,x} - 2\dot{\varepsilon}_c \dot{v}_{,x} - \ddot{\varepsilon}_c v_{,x} \tag{33}$$

$$\ddot{\varepsilon}_c = \frac{1}{L}(\mathbf{G}_a^t \ddot{\mathbf{u}}_a + \dot{\mathbf{G}}_b^t \dot{\mathbf{u}}_b + \mathbf{G}_b^t \ddot{\mathbf{u}}_b) \tag{34}$$

### 2.5. Element nodal force vector

Let $\delta u_j$ and $\delta v_j$, and $\delta\theta_j$ ($j=1, 2$) denote the virtual displacements in the $x_1$ and $x_2$ directions of the current inertia element coordinates, and virtual rotations applied at the element nodes $j$. The element nodal force corresponding to virtual nodal displacement $\delta u_j$ and $\delta v_j$, and $\delta\theta_j$ ($j=1, 2$) are $f_{ij}$, the forces in the $x_i$ ($i=1, 2$) directions, and $m_j$ moments about the $x_3$ axis, at element local nodes $j$.

The element nodal force vector is obtained from the d'Alembert principle and the virtual work principle in the current inertia element coordinates. The virtual work principle requires that

$$\delta\mathbf{u}_a^t \mathbf{f}_a + \delta\mathbf{u}_b \mathbf{f}_b = \int_V (\delta\varepsilon_{11}\sigma_{11} + \rho\delta\mathbf{r}^t\ddot{\mathbf{a}})dV \tag{35}$$

$$\delta\mathbf{u}_a = \{\delta u_1, \delta u_2\} \tag{36}$$

$$\delta\mathbf{u}_b^\theta = \{\delta v_1, \delta\theta_1, \delta v_2, \delta\theta_2\} \tag{37}$$

$$\mathbf{f}_a = \mathbf{f}_a^D + \mathbf{f}_a^I = \{f_{11}, f_{12}\} \tag{38}$$

$$\mathbf{f}_b = \mathbf{f}_b^D + \mathbf{f}_b^I = \{f_{21}, m_1, f_{22}, m_2\} \tag{39}$$

$$\mathbf{f}_a^D = \{f_{11}^D, f_{12}^D\} \tag{40}$$

$$\mathbf{f}_b^D = \{f_{21}^D,\ m_1^D,\ f_{22}^D,\ m_2^D\} \tag{41}$$

$$\mathbf{f}_a^I, = \{f_{11}^I,\ f_{22}^I\} \tag{42}$$

$$\mathbf{f}_b^I, = \{f_{21}^I,\ m_1^I,\ f_{22}^I,\ m_2^I\} \tag{43}$$

where $\mathbf{f}_i$ ($i=a, b$) are the generalized force vectors corresponding to $\delta\mathbf{u}_a$ and $\delta\mathbf{u}_b^\theta$, $\mathbf{f}_i^D$ and $\mathbf{f}_i^I$ ($i=a, b$) are element deformation nodal force vector and inertia nodal force vector corresponding to $\mathbf{f}_i$, respectively, $V$ is the volume of the undeformed beam element, $\delta\varepsilon_{11}$ is the variation of $\varepsilon_{11}$ in Eq. (19) corresponding to $\delta\boldsymbol{u}_a$ and $\delta\mathbf{u}_b^\theta$. $\sigma_{11}$ is the engineering stress. For linear elastic material, $\sigma_{11}=E\varepsilon_{11}$, where $E$ is Young's modulus. $\rho$ is the density, $\delta\mathbf{r}$ is the variation of $\boldsymbol{r}$ in Eq. (15) corresponding to $\delta\mathbf{u}_a$ and $\delta\mathbf{u}_b^\theta$, and $\mathbf{a}$ is the absolute acceleration in Eq. (21). Note that $\delta\varepsilon_{11}$ and $\delta\mathbf{u}_a$ are functions of $\delta\mathbf{u}_a$ and $\delta\mathbf{u}_b$. However, the difference between $\delta\theta$ and $\delta v'$ is considered here. Thus, the relation between $\delta\mathbf{u}_b^\theta$, $\delta\mathbf{u}_a$ and $\delta\mathbf{u}_b$ is required, and will be derived later in this section.

If the element size is chosen to be sufficiently small, the values of the deformation parameters of the deformed element defined in the current element coordinate system may always be much smaller than unity. Thus the higher-order terms of deformation parameters in the element internal nodal forces may be neglected. However, in order to include the nonlinear coupling among the bending and stretching deformations, the terms up to the second order of deformation parameters and their spatial derivatives are retained in element deformation nodal forces by consistent second-order linearization of $\delta\varepsilon_{11}\sigma_{11}$ in Eq. (35). Here, only infinitesimal free vibration is considered, thus only the terms up to the first order of time derivatives of deformation parameters and their spatial derivatives are retained in element inertia nodal forces by consistent first-order linearization of $\delta\mathbf{r}^t\ddot{\mathbf{a}}$ in Eq. (35). Note that the values of $L$, $v$ and $v_{,x}$ will converge to zero, and the values of $v_{,x}/L$, $\varepsilon_c$ and $v_{,xx}$ will converge to constants

with the decrease of the element size. Thus, the higher order terms containing $L$, $v$, and $v_{,x}$ are neglected, and the higher order terms containing $v_{,x}/L$, $\varepsilon_c$ and $v_{,xx}$ are retained in the element internal nodal forces here. However, to avoid improper omission in the element internal nodal forces in this section and element matrices in the next section, some third order terms are retained in the derivation process.

From Eqs. (6) and (11)–(14), the variation of $\varepsilon_{11}$ in Eq. (19) may be expressed as

$$\delta\varepsilon_{11} = \delta\varepsilon_c + yv_{,xx}\delta\varepsilon_c - (1-\varepsilon_c)y\delta v_{,xx} \tag{44}$$

$$\delta\varepsilon_c = \frac{1}{L}(\delta\mathbf{u}_a^t\mathbf{G}_a + \delta\mathbf{u}_b^t\mathbf{G}_b) \tag{45}$$

$$\delta v_{,xx} = \delta\mathbf{u}_b^t\mathbf{N}_b'' \tag{46}$$

From Eqs. (6) and (15)–(18), $\delta\mathbf{r}$ the variation of $\mathbf{r}$ in Eq. (15) may be expressed as

$$\delta\mathbf{r} = \{\delta r_1, \delta r_2, 0\} = \{\delta x_p - y\delta\theta, \delta v - y\theta\delta\theta, 0\} \tag{47}$$

$$\delta x_p = \delta\mathbf{u}_a^t\mathbf{N}_a + \frac{x}{L}\delta\mathbf{u}_b^t\mathbf{G}_b - \int_0^x v_{,x}\delta v_{,x}\,dx \tag{48}$$

$$\delta\theta = -\delta\varepsilon_c v_{,x} + (1-\varepsilon_c)\delta v_{,x} \tag{49}$$

$$\delta v_{,x} = \delta\mathbf{u}_b^t\mathbf{N}_b' \tag{50}$$

From Eqs. (45), (49) and (50), the relations between $\delta\mathbf{u}_b$ in Eq. (46) or (50) and $\delta\mathbf{u}_b^\theta$ in Eq. (37) may be expressed as

$$\delta\mathbf{u}_b = \mathbf{T}_b\delta\mathbf{u}_b^\theta + \mathbf{T}_{ba}\delta\mathbf{u}_a \tag{51}$$

$$\mathbf{T}_b = \mathbf{T}_b^1 + \mathbf{T}_b^2 \tag{52}$$

$$\mathbf{T}_b^1 = \begin{bmatrix} 1 & 0 & 0 & 0 \\ 0 & 1+\varepsilon_c & 0 & 0 \\ 0 & 0 & 1 & 0 \\ 0 & 0 & 0 & 1+\varepsilon_c \end{bmatrix} \tag{53}$$

$$\mathbf{T}_b^2 = [\mathbf{0}_{4\times1}, v_1'\mathbf{G}_b, \mathbf{0}_{4\times1}, v_2'\mathbf{G}_b]^t \tag{54}$$

$$\mathbf{T}_{ba} = \begin{bmatrix} 0 & 0 \\ \dfrac{-v_1'}{L} & \dfrac{v_1'}{L} \\ 0 & 0 \\ \dfrac{-v_2'}{L} & \dfrac{v_2'}{L} \end{bmatrix} \tag{55}$$

Substituting Eqs. (21)–(34) and (44)–(55) into Eq. (35), using $\int y\,dA = 0$, neglecting the higher order terms, we may obtain

$$\mathbf{f}_a^D = EA\varepsilon_c\mathbf{G}_a - \frac{EI\varepsilon_c}{L}\int v_{,xx}^2\,dx\mathbf{G}_a \tag{56}$$

$$\mathbf{f}_b^D = \mathbf{T}_b^{1t}\left[EI(1-\varepsilon_c)^2\int \mathbf{N}_b''v_{,xx}\,dx + f_{12}^D\int \mathbf{N}_b'v_{,x}\,dx\right] \tag{57}$$

$$\mathbf{f}_a^I = \rho A\int \mathbf{N}_a\mathbf{N}_a^t\,dx\ddot{\mathbf{u}}_a + \underline{\Omega^2\rho A a_{o1}\int \mathbf{N}_a\,dx} - \underline{\Omega^2\rho A\int \mathbf{N}_a(\mathbf{N}_a^t\mathbf{u}_a + x)dx} - 2\Omega\rho A\int \mathbf{N}_a\dot{v}\,dx \tag{58}$$

$$\mathbf{f}_b^I = \mathbf{T}_b^{1t}\left[\rho A\int \mathbf{N}_b\ddot{v}\,dx + \rho I(1-\varepsilon_c)^2\int \mathbf{N}_b'\ddot{v}_{,x}\,dx + \underline{\Omega^2\rho A a_{o2}\int \mathbf{N}_b\,dx} - \underline{\Omega^2\rho A\int \mathbf{N}_b v\,dx} - \underline{\Omega^2\rho I\int \mathbf{N}_b'v'\,dx} + 2\Omega\rho A\int \mathbf{N}_b\mathbf{N}_a^t\,dx\dot{\mathbf{u}}_a\right] \tag{59}$$

where the range of integration for the integral $\int(\,)dx$ in Eqs. (56)–(59) is from 0 to $L$, $A$ is the cross section area, $I$ is moment of inertia of the cross section, $a_{oi}$ $(i=1,2)$ are the $x_i$ components of $\mathbf{a}_o$ in Eq. (23). The underlined terms in Eqs. (58) and (59) are the inertia nodal force corresponding to the steady state deformation induced by the constant rotation.

### 2.6. Element matrices

The element matrices considered are element tangent stiffness matrix, mass matrix, centripetal stiffness matrix and gyroscopic matrix. The element matrices may be obtained by differentiating the element nodal force vectors in Eqs. (56)–(59) with respect to nodal parameters, and time derivatives of nodal parameters.

Using the direct stiffness method, the element tangent stiffness matrix may be assembled by the following submatrices:

$$\mathbf{k}_{aa} = \frac{\partial\mathbf{f}_a^D}{\partial\mathbf{u}_a} = \left(\frac{EA}{L} - \frac{EI}{L^2}\int v_{,xx}^2\,dx\right)\mathbf{G}_a\mathbf{G}_a^t \tag{60}$$

$$\mathbf{k}_{ab} = \mathbf{k}_{ba}^t = \frac{\partial\mathbf{f}_a^D}{\partial\mathbf{u}_b^\theta} = -\frac{2EI\varepsilon_c}{L}\mathbf{G}_a\int v_{,xx}\mathbf{N}_b''^t\,dx\mathbf{T}_b^1 \tag{61}$$

$$\mathbf{k}_{bb} = \frac{\partial\mathbf{f}_b^D}{\partial\mathbf{u}_b^\theta} = \mathbf{T}_b^{1t}\left[EI(1-\varepsilon_c)^2\int \mathbf{N}_b''\mathbf{N}_b''^t\,dx + f_{12}^D\int \mathbf{N}_b'\mathbf{N}_b''^t\,dx\right]\mathbf{T}_b^1 \tag{62}$$

The element mass matrix may be assembled by the following submatrices:

$$\mathbf{m}_{aa} = \frac{\partial\mathbf{f}_a^I}{\partial\ddot{\mathbf{u}}_a} = \rho A\int \mathbf{N}_a\mathbf{N}_a^t\,dx \tag{63}$$

$$\mathbf{m}_{ab} = \mathbf{m}_{ba}^t = \frac{\partial\mathbf{f}_a^I}{\partial\ddot{\mathbf{u}}_b^\theta} = \mathbf{0} \tag{64}$$

$$\mathbf{m}_{bb} = \frac{\partial\mathbf{f}_b^I}{\partial\ddot{\mathbf{u}}_b^\theta} = \mathbf{T}_b^{1t}\left[\rho A\int \mathbf{N}_b\mathbf{N}_b^t\,dx + \rho I(1-\varepsilon_c)^2\int \mathbf{N}_b'\mathbf{N}_b''^t\,dx\right]\mathbf{T}_b^1 \tag{65}$$

The element centripetal stiffness matrix may be assembled by the following submatrices:

$$\mathbf{k}_{\Omega aa} = \frac{\partial\mathbf{f}_a^I}{\Omega^2\partial\mathbf{u}_a} = -\rho A\int \mathbf{N}_a\mathbf{N}_a^t\,dx \tag{66}$$

$$\mathbf{k}_{\Omega ab} = \mathbf{k}_{\Omega ab}^t = \frac{\partial\mathbf{f}_a^I}{\Omega^2\partial\mathbf{u}_b^\theta} = \mathbf{0} \tag{67}$$

$$\mathbf{k}_{\Omega bb} = \frac{\partial\mathbf{f}_b^I}{\Omega^2\partial\mathbf{u}_b^\theta} = \mathbf{T}_b^{1t}\left[-\rho A\int \mathbf{N}_b\mathbf{N}_b^t\,dx\right]\mathbf{T}_b^1 \tag{68}$$

The element gyroscopic matrix may be assembled by the following submatrices:

$$\mathbf{c}_{aa} = \frac{\partial\mathbf{f}_a^I}{\Omega\partial\dot{\mathbf{u}}_a} = \mathbf{0} \tag{69}$$

$$\mathbf{c}_{ab} = -\mathbf{c}_{ba}^t = \frac{\partial\mathbf{f}_a^I}{\Omega\partial\dot{\mathbf{u}}_b^\theta} = -2\rho A\int \mathbf{N}_a\mathbf{N}_b^t\,dx\mathbf{T}_b^1 \tag{70}$$

$$\mathbf{c}_{bb} = \frac{\partial\mathbf{f}_b^I}{\Omega\partial\dot{\mathbf{u}}_b} = \mathbf{0} \tag{71}$$

### 2.7. Equations of motion

For convenience, the following dimensionless variables are used:

$$\overline{x}=\frac{x}{L_T},\quad \overline{R}=\frac{R}{L_T},\quad \overline{X}_o=\frac{X_o}{L_T},\quad \overline{Y}_o=\frac{Y_o}{L_T},$$
$$\overline{L}=\frac{L}{L_T},\quad \overline{u}=\frac{u}{L_T},\quad \overline{v}=\frac{v}{L_T} \tag{72}$$

$$\overline{u}'=\frac{\partial\overline{u}}{\partial\overline{x}}=u',\quad \overline{u}''=\frac{\partial^2\overline{u}}{\partial\overline{x}^2}=L_T u'',\quad \overline{v}'=\frac{\partial\overline{v}}{\partial\overline{x}}=v',\quad \overline{v}''=\frac{\partial^2\overline{v}}{\partial\overline{x}^2}=L_T v''$$

$$\overline{f}_{ij}=\frac{f_{ij}}{EA},\quad \overline{m}_j=\frac{m_j}{EAL_T},\quad (i=1,2;j=1,2)$$

$$\tau=\frac{t}{L_T}\sqrt{\frac{E}{\rho}},\quad \dot{\overline{u}}=\frac{\partial\overline{u}}{\partial\tau}=\dot{u}\sqrt{\frac{\rho}{E}},\quad \ddot{\overline{u}}=\frac{\partial^2\overline{u}}{\partial\tau^2}=L_T\frac{\rho}{E}\ddot{u}$$

$$\dot{\overline{v}}=\frac{\partial\overline{v}}{\partial\tau}=\dot{v}\sqrt{\frac{\rho}{E}},\quad \ddot{\overline{v}}=\frac{\partial^2\overline{v}}{\partial\tau^2}=L_T\frac{\rho}{E}\ddot{v}$$

$$k=\Omega L_T\sqrt{\frac{\rho}{E}},\quad K=\omega L_T\sqrt{\frac{\rho}{E}},\quad \overline{I}=\frac{I}{AL_T^2}=\frac{1}{\eta^2}$$

where $E$ is Young's modulus, $\rho$ is the density, $\tau$ is a dimensionless time, $\Omega$ and $k$ are angular speed and a dimensionless angular speed of rotating beam, respectively, $\omega$ and $K$ are natural frequency and dimensionless natural frequency of rotating beam, respectively, and $\eta$ is the slenderness ratio of the rotating beam.

The dimensionless nonlinear equations of motion for a rotating beam with constant angular velocity may be expressed by

$$\boldsymbol{\varphi}=\mathbf{F}^D(\widehat{\mathbf{Q}})+\mathbf{F}^I(k^2,\widehat{\mathbf{Q}},\dot{\widehat{\mathbf{Q}}},\ddot{\widehat{\mathbf{Q}}})=\mathbf{0} \tag{73}$$

$$\widehat{\mathbf{Q}}=\mathbf{Q}_s+\mathbf{Q}(\tau) \tag{74}$$

where $\boldsymbol{\varphi}$, $\boldsymbol{F}^D$ and $\boldsymbol{F}^I$ are the dimensionless unbalanced force vector, the dimensionless deformation nodal force vector and the dimensionless inertia nodal force vector of the structural system, respectively. $\mathbf{F}^I$ and $\mathbf{F}^D$ are assembled from the dimensionless element nodal force vectors, which are calculated using Eqs. (56)–(59) and (72) first in the current element coordinates and then transformed from element coordinate system to global coordinate system before assemblage using standard procedure. $\widehat{\mathbf{Q}}$ is the dimensionless nodal displacement vector of the rotating beam, $\dot{\widehat{\mathbf{Q}}}=\partial\widehat{\mathbf{Q}}/\partial\tau$ and $\ddot{\widehat{\mathbf{Q}}}=\partial^2\widehat{\mathbf{Q}}/\partial\tau^2$ are the dimensionless nodal velocity vector and the dimensionless nodal acceleration vector of the rotating beam, respectively, $\mathbf{Q}_s$ is the dimensionless steady state nodal displacement vector induced by constant dimensionless rotation speed $k$, $\mathbf{Q}(\tau)$ is the time-dependent dimensionless nodal displacements vector caused by the free vibration of the rotating beam. Here only infinitesimal vibration is considered.

### 2.8. Governing equations for steady state deformation

For the steady-state deformations, $\mathbf{Q}(\tau)=\mathbf{0}$. Thus Eq. (73) can be reduced to nonlinear dimensionless steady state equilibrium equations and expressed by

$$\boldsymbol{\varphi}=\mathbf{F}_s^D(\mathbf{Q}_s)+k^2\mathbf{F}_s^I(\mathbf{Q}_s)=\mathbf{0} \tag{75}$$

where $\mathbf{F}_s^D(\mathbf{Q}_s)$ and $k^2\mathbf{F}_s^I(\mathbf{Q}_s)$ are the dimensionless deformation nodal force vector and the dimensionless inertia nodal force (the centrifugal force) vector of the structural system corresponding to the dimensionless steady state nodal displacement vector $\mathbf{Q}_s$, respectively. $k^2\mathbf{F}_s^I(\mathbf{Q}_s)$ is corresponding to the underlined terms of Eqs. (58) and (59). Note that $k^2\mathbf{F}_s^I(\mathbf{Q}_s)$ is deformation dependent. Thus $k^2\mathbf{F}_s^I(\mathbf{Q}_s)$ should be updated at each new configuration.

Here, an incremental-iterative method based on the Newton–Raphson method is employed for the solution of nonlinear dimensionless steady state equilibrium equations at different dimensionless rotation speed $k$. In this paper, a weighted Euclidean norm of the unbalanced force is employed for the equilibrium

**Table 1**
Comparison of results for different cases ($\eta=20$, $\overline{R}=1.5$).

| $\alpha$ (deg.) | $k$ | | $\varepsilon_c^{\max}$ ($10^{-3}$) | $\varepsilon_b^{\max}$ ($10^{-3}$) | $v_{tip}/L_T$ ($10^{-3}$) | $K_1$ | $K_2$ | $K_3$ ($a$) | $K_4$ | $K_5$ | $K_6$ | $K_7$ ($a$) |
|---|---|---|---|---|---|---|---|---|---|---|---|---|
| 0 | 0 | EA10 | 0 | 0 | 0 | .174788 | 1.05957 | 1.57241 | 2.82495 | 4.75610 | 5.19546 | 8.00214 |
| | | EA50 | 0 | 0 | 0 | .174787 | 1.05953 | 1.57086 | 2.82431 | 4.71413 | 5.19120 | 7.86206 |
| | | EA100 | 0 | 0 | 0 | .174787 | 1.05953 | 1.57081 | 2.82431 | 4.71283 | 5.19119 | 7.85600 |
| | | [23] | 0 | 0 | 0 | .17479 | 1.05953 | 1.57080 | 2.82431 | 4.71239 | 5.19119 | – |
| | | [31] | 0 | 0 | 0 | .17580 | 1.10172 | 1.57080 | 3.08486 | 4.71239 | 6.04510 | – |
| | .06 | EA10 | 6.93309 | 0 | 0 | .197994 | 1.08369 | 1.57615 | 2.84311 | 4.75729 | 5.20566 | 8.00257 |
| | | EA50 | 7.15492 | 0 | 0 | .197894 | 1.08337 | 1.57461 | 2.84191 | 4.71534 | 5.19999 | 7.86273 |
| | | EA100 | 7.18210 | 0 | 0 | .197891 | 1.08336 | 1.57456 | 2.84190 | 4.71403 | 5.19994 | 7.85667 |
| | | EB100 | 7.18210 | 0 | 0 | .198511 | 1.08726 | 1.57457 | 2.85242 | 4.71403 | 5.21930 | 7.85669 |
| | | [23] | 7.20000 | 0 | 0 | .19862 | 1.08760 | 1.57455 | 2.85276 | 4.71360 | 5.21962 | – |
| | | LAS | 7.20000 | 0 | 0 | – | – | – | – | – | – | – |
| 5 | .03 | EA10 | 1.72680 | 1.93655 | 5.48934 | .180882 | 1.06562 | 1.57335 | 2.82949 | 4.75639 | 5.19801 | 8.00220 |
| | | EA50 | 1.78195 | 1.94115 | 5.49004 | .180854 | 1.06552 | 1.57180 | 2.82871 | 4.71442 | 5.19339 | 7.86221 |
| | | EA100 | 1.78871 | 1.94131 | 5.49007 | .180853 | 1.06552 | 1.57175 | 2.82871 | 4.71312 | 5.19337 | 7.85615 |
| | | EB100 | 1.78870 | 1.93560 | 5.47701 | .181020 | 1.06651 | 1.57175 | 2.83136 | 4.71312 | 5.19822 | 7.85616 |
| | | LAS | 1.79486 | 2.03794 | 5.88301 | – | – | – | – | – | – | – |
| 30 | .01 | EA10 | .173298 | 1.29046 | 3.72389 | .175392 | 1.06018 | 1.57252 | 2.82541 | 4.75613 | 5.19573 | 8.00213 |
| | | EA50 | .178615 | 1.29263 | 3.72394 | .175389 | 1.06014 | 1.57097 | 2.82476 | 4.71416 | 5.19142 | 7.86207 |
| | | EA100 | .179264 | 1.29270 | 3.72395 | .175389 | 1.06014 | 1.57092 | 2.82476 | 4.71285 | 5.19141 | 7.85601 |
| | | EB100 | .179264 | 1.29231 | 3.72300 | .175407 | 1.06024 | 1.57092 | 2.82503 | 4.71285 | 5.19190 | 7.85601 |
| | | LAS | .179904 | 1.29904 | 3.75000 | – | – | – | – | – | – | – |
| 90 | .01 | EA10 | .0500346 | 2.59388 | 7.49567 | .174830 | 1.05974 | 1.57253 | 2.82511 | 4.75612 | 5.19557 | 8.00206 |
| | | EA50 | .0500385 | 2.59808 | 7.49570 | .174829 | 1.05971 | 1.57098 | 2.82447 | 4.71415 | 5.19128 | 7.86205 |
| | | EA100 | .0500217 | 2.59821 | 7.49570 | .174829 | 1.05971 | 1.57093 | 2.82447 | 4.71284 | 5.19127 | 7.85599 |
| | | EB100 | .0500216 | 2.59797 | 7.49507 | .174835 | 1.05974 | 1.57093 | 2.82456 | 4.71284 | 5.19144 | 7.85599 |
| | | LAS | .0500000 | 2.59807 | 7.50000 | – | – | – | – | – | – | – |

iterations, and is given by

$$\frac{\|\boldsymbol{\varphi}\|}{k^2\sqrt{N}\|\mathbf{F}_s^I\|} \le e_{tol} \tag{76}$$

where $N$ is number of the equations of the system, and $e_{tol}$ is a prescribed value of error tolerance. Unless otherwise stated, the error tolerance $e_{tol}$ is set to $10^{-5}$ in this study.

### 2.9. Governing equations for free vibration measured from the position of steady state deformation

Substituting Eq. (74) into Eq. (73), and setting the first-order Taylor series expansion of the unbalanced force vector $\boldsymbol{\varphi}$ around $\mathbf{Q}_s$ to zero, one may obtain the dimensionless governing equations for linear free vibration of the rotating beam measured from the

**Table 2**
Comparison of results for different cases ($\eta=100$, $\overline{R}=1.5$).

| $\alpha$ (deg.) | $k$ | | $\varepsilon_c^{max}$ ($10^{-3}$) | $\varepsilon_b^{max}$ ($10^{-3}$) | $v_{tip}/L_T$ | $K_1$ ($10^{-1}$) | $K_2$ | $K_3$ | $K_4$ | $K_5$ ($a$) | $K_6$ | $K_7$ |
|---|---|---|---|---|---|---|---|---|---|---|---|---|
| 0 | 0 | EA10 | 0 | 0 | 0 | .351520 | .219996 | .614757 | 1.20161 | 1.57241 | 1.98111 | 2.95267 |
| | | EA50 | 0 | 0 | 0 | .351520 | .219989 | .614602 | 1.20047 | 1.57086 | 1.97619 | 2.93707 |
| | | EA100 | 0 | 0 | 0 | .351520 | .219989 | .614601 | 1.20047 | 1.57081 | 1.97618 | 2.93704 |
| | | [23] | 0 | 0 | 0 | .3515 | .21999 | .61460 | 1.20047 | 1.57080 | 1.97618 | – |
| | | [31] | 0 | 0 | 0 | .3516 | .22034 | .616972 | 1.20902 | 1.57080 | – | – |
| | .06 | EA10 | 6.93309 | 0 | 0 | 1.00061 | .337850 | 753355 | 1.35311 | 1.57588 | 2.13851 | 3.11190 |
| | | EA50 | 7.15492 | 0 | 0 | .999008 | .336839 | .751962 | 1.35058 | 1.57434 | 2.13195 | 3.09426 |
| | | EA100 | 7.18210 | 0 | 0 | .998959 | .336808 | .751924 | 1.35054 | 1.57429 | 2.13188 | 3.09415 |
| | | EB100 | 7.18210 | 0 | 0 | .999710 | .337324 | .753756 | 1.35450 | 1.57429 | 2.13877 | 3.10471 |
| | | [23] | 7.20000 | 0 | 0 | .9989 | .33722 | .75363 | 1.35435 | 1.57427 | 2.13860 | – |
| | | LAS | 7.20000 | 0 | 0 | – | – | – | – | – | – | – |
| 5 | .03 | EA10 | 1.72775 | 5.09357 | .0511913 | .591219 | .254778 | .652135 | 1.24001 | 1.57551 | 2.02262 | 2.99338 |
| | | EA50 | 1.78184 | 5.17548 | .0512390 | .590437 | .254476 | .651668 | 1.23856 | 1.57386 | 2.01728 | 2.97726 |
| | | EA100 | 1.78842 | 5.17847 | .0512404 | .590413 | .254467 | .651657 | 1.23855 | 1.57381 | 2.01725 | 2.97721 |
| | | EB100 | 1.78840 | 5.16732 | .0511903 | .590651 | .254646 | .652209 | 1.23966 | 1.57382 | 2.01911 | 2.97999 |
| | | LAS | 1.79486 | 10.1897 | .1470753 | – | – | – | – | – | – | – |
| 30 | .01 | EA10 | .174250 | 5.74549 | .0788668 | .383279 | .223645 | .617615 | 1.20301 | 1.57860 | 1.98709 | 2.95692 |
| | | EA50 | .178734 | 5.76488 | .0788899 | .383144 | .223606 | .617430 | 1.20185 | 1.57696 | 1.98213 | 2.94126 |
| | | EA100 | .179264 | 5.76552 | .0788906 | .383140 | .223605 | .617428 | 1.20185 | 1.57691 | 1.98212 | 2.94123 |
| | | EB100 | .179262 | 5.76388 | .0788731 | .383173 | .223626 | .617490 | 1.20197 | 1.57691 | 1.98231 | 2.94152 |
| | | LAS | .179904 | 6.49519 | .0937500 | – | – | – | – | – | – | – |
| 90 | .01 | EA10 | .0543132 | 12.7940 | .179785 | .361111 | .220583 | .610488 | 1.19029 | 1.60306 | 1.99241 | 295467 |
| | | EA50 | .0504783 | 12.8203 | .179801 | .361062 | .220567 | .610327 | 1.18916 | 1.60109 | 1.98747 | 293903 |
| | | EA100 | .0499228 | 12.8211 | .179801 | .361060 | .220566 | .610327 | 1.18916 | 1.60104 | 1.98745 | 293899 |
| | | EB100 | .0499202 | 12.8198 | .179783 | .361076 | .220576 | .610354 | 1.18921 | 1.60105 | 1.98753 | 293912 |
| | | LAS | .0500000 | 12.9904 | .187500 | – | – | – | – | – | – | – |

**Table 3**
Comparison of results for different cases ($\eta=1000$, $\overline{R}=1.5$).

| $\alpha$ (deg.) | $k$ | | $\varepsilon_c^{max}$ ($10^{-3}$) | $\varepsilon_b^{max}$ ($10^{-3}$) | $v_{tip}/L_T$ | $K_1$ ($10^{-2}$) | $K_2$ ($10^{-1}$) | $K_3$ ($10^{-1}$) | $K_4$ | $K_5$ | $K_6$ | $K_7$ |
|---|---|---|---|---|---|---|---|---|---|---|---|---|
| 0 | 0 | EA10 | 0 | 0 | 0 | .351601 | .220349 | .617105 | .121008 | .200340 | .300117 | .421052 |
| | | EA50 | 0 | 0 | 0 | .351601 | .220341 | .616949 | .120893 | .199838 | .298509 | .416903 |
| | | EA100 | 0 | 0 | 0 | .351601 | .220341 | .616948 | .120893 | .199837 | .298506 | .416896 |
| | | [23] | 0 | 0 | 0 | .352 | .2203 | .6169 | .12089 | .19984 | .29851 | – |
| | | [31] | 0 | 0 | 0 | .3516 | .22034 | .616972 | .120902 | – | – | – |
| | .06 | EA10 | 6.93309 | 0 | 0 | 9.00392 | 2.50170 | 4.13382 | .591357 | .784564 | .992667 | 1.21721 |
| | | EA50 | 7.15492 | 0 | 0 | 8.96171 | 2.47409 | 4.06028 | .580433 | .771135 | .975828 | 1.19320 |
| | | EA100 | 7.18210 | 0 | 0 | 8.96090 | 2.47299 | 4.05718 | .580000 | .770663 | .975346 | 1.19271 |
| | | EB100 | 7.18210 | 0 | 0 | 8.96152 | 2.47312 | 4.05756 | .580088 | .770833 | .975634 | 1.19316 |
| | | [23] | 7.20000 | 0 | 0 | 8.952 | 2.4708 | 4.0536 | .57955 | .77017 | .97486 | – |
| | | LAS | 7.20000 | 0 | 0 | – | – | – | – | – | – | – |
| 5 | .03 | EA10 | 1.73113 | 3.88613 | .0835235 | 4.54694 | 1.27442 | 2.17642 | .323061 | .442957 | .577154 | .726538 |
| | | EA50 | 1.78397 | 6.01548 | .0838255 | 4.53331 | 1.26216 | 2.15013 | .319740 | .439096 | .572342 | .719773 |
| | | EA100 | 1.78938 | 6.21315 | .0838279 | 4.53304 | 1.26175 | 2.14927 | .319641 | .438996 | .572245 | .719680 |
| | | EB100 | 1.78936 | 6.20203 | .0838218 | 4.53320 | 1.26179 | 2.14942 | .319678 | .439068 | .572368 | .719873 |
| | | LAS | 1.79486 | 101.897 | 14.70753 | – | – | – | – | – | – | – |
| 30 | .008 | EA10 | .117176 | 8.73688 | .429697 | 1.29066 | .405573 | .836364 | .143457 | .221474 | .319570 | .439088 |
| | | EA50 | .114344 | 9.36265 | .429987 | 1.28846 | .404148 | .836039 | .143625 | .221421 | .318236 | .434627 |
| | | EA100 | .113413 | 9.38899 | .429994 | 1.28839 | .404101 | .836030 | .143637 | .221447 | .318271 | .434665 |
| | | EB100 | .113410 | 9.38784 | .429986 | 1.28840 | .404108 | .836056 | .143643 | .221458 | .318289 | .434691 |
| | | LAS | .115138 | 41.5692 | 6.00000 | – | – | – | – | – | – | – |
| 90 | .003 | EA10 | .00632598 | 8.11019 | .747141 | .561366 | .232167 | .566047 | .113316 | .190888 | .289635 | .409720 |
| | | EA50 | .00388231 | 8.15303 | .747254 | .560584 | .232181 | .566295 | .113203 | .190324 | .287893 | .405356 |
| | | EA100 | .00351746 | 8.15402 | .747257 | .560557 | .232180 | .566302 | .113202 | .190320 | .287884 | .405339 |
| | | EB100 | .00351740 | 8.15396 | .747254 | .560558 | .232181 | .566306 | .113202 | .190322 | .287886 | .405342 |
| | | LAS | .00450000 | 11.6913 | 1.68750 | – | – | – | – | – | – | – |

position of the steady-state deformation as follows:

$$\mathbf{M}\ddot{\mathbf{Q}}+\mathbf{C}\dot{\mathbf{Q}}+(\mathbf{K}+k^2\mathbf{K}_\Omega)\mathbf{Q}=\mathbf{0} \tag{77}$$

where **M**, **C**, **K** and $\mathbf{K}_\Omega$ are dimensionless mass matrix, gyroscopic matrix, tangent stiffness matrix and centripetal stiffness matrix of the rotating beam, respectively. **M**, **C**, **K**, and $\mathbf{K}_\Omega$ are assembled from the dimensionless element mass matrix, gyroscopic matrix, tangent stiffness matrix and centripetal stiffness matrix, which are calculated using Eqs. (60)–(72) first in the current element coordinates and then transformed from element coordinate system to global coordinate system before assemblage using standard procedure.

We shall seek a solution of Eq. (77) in the form

$$\mathbf{Q}=(\mathbf{Q}_R+i\mathbf{Q}_I)e^{iK\tau} \tag{78}$$

where $i=\sqrt{-1}$, $K$ and $\tau$ are dimensionless natural frequency of rotating beam and dimensionless time defined in Eq. (72), and $\mathbf{Q}_R$ and $\mathbf{Q}_I$ are real part and imaginary part of the vibration mode.

Substituting Eq. (78) into Eq. (77), one may obtain a set of homogeneous equations expressed by

$$\mathbf{HZ}=\mathbf{0} \tag{79}$$

$$\mathbf{H}=\mathbf{H}(K,k)=\begin{bmatrix}\mathbf{K}+k^2\mathbf{K}_\Omega-K^2\mathbf{M} & kK\mathbf{C}^t\\ kK\mathbf{C} & \mathbf{K}+k^2\mathbf{K}_\Omega-K^2\mathbf{M}\end{bmatrix} \tag{80}$$

$$\mathbf{Z}=\{\mathbf{Q}_R,\mathbf{Q}_I\} \tag{81}$$

where $\mathbf{H}(K,k)$ denotes **H** is a function of $K$ and $k$. Note that **H** is a symmetric matrix.

Eq. (79) is a quadratic eigenvalue problem. For a nontrivial **Z**, the determinant of matrix **H** in Eq. (79) must be equal to zero. The values of $K$, which make the determinant vanish, are called eigenvalues of matrix **H**. The bisection method is used here to find the eigenvalues. Note that when $k=0$, Eq. (79) will degenerate to a generalized eigenvalue problem.

**Table 4**
Dimensionless frequencies for rotating beam with different inclination angle ($\eta=70$, $\overline{R}=1$, $k=5/70$).

| $\alpha$ (deg.) | $\varepsilon_c^{\max}$ ($10^{-3}$) | | $\varepsilon_b^{\max}$ | $v_{tip}/L^T$ | $K_1$ | | | $K_2$ | | |
|---|---|---|---|---|---|---|---|---|---|---|
| | EA | EC | EA | EA | EA | EC | [20] | EA | EC | [20] |
| 0 | 7.61579 | 7.61579 | 0 | 0 | .105427 | .105427 | .105 | .410792 | .410792 | .418 |
| 10 | 7.53381 | 7.53893 | .0220374 | .119890 | .105377 | .104869 | .105 | .410400 | .410001 | .417 |
| 20 | 7.28963 | 7.31066 | .0438841 | .237606 | .105225 | .103195 | .103 | .409219 | .407642 | .414 |
| 30 | 6.88882 | 6.93792 | .0653510 | .351025 | .104971 | .100399 | .100 | .407246 | .403758 | .410 |
| 40 | 6.34057 | 6.43205 | .0862526 | .458121 | .104612 | .0964721 | .096 | .404475 | .398421 | .405 |
| 50 | 5.65758 | 5.80840 | .106408 | .557013 | .104146 | .0913941 | .091 | .400900 | .391733 | .398 |
| 60 | 4.85594 | 5.08596 | .125641 | .646008 | .103568 | .0851262 | .085 | .396518 | .383830 | .390 |
| 70 | 3.95486 | 4.28663 | .143786 | .723643 | .102875 | .0775919 | .077 | .391331 | .374876 | .381 |
| 80 | 2.97641 | 3.43472 | .160683 | .788722 | .102058 | .0686418 | .068 | .385349 | .365073 | .371 |
| 90 | 1.94513 | 2.55611 | .176180 | .840342 | .101109 | .0579597 | .057 | .378595 | .354659 | .361 |

$k=0$, $K_1=.0502050$, $K_2=.313742$.

**Table 5**
Dimensionless frequencies for rotating beam with different inclination angle ($\eta=100$, $\overline{R}=1$, $k=.01$).

| $\alpha$ (deg.) | $\varepsilon_c^{\max}$ ($10^{-3}$) | | $\varepsilon_b^{\max}$ ($10^{-3}$) | $v_{tip}/L_T$ | $K_1$ ($10^{-1}$) | | $K_2$ | | $K_3$ | | $K_4$ | |
|---|---|---|---|---|---|---|---|---|---|---|---|---|
| | EA | EC | EA | EA | EA | EC | EA | EC | EA | EC | EA | EC |
| 0 | .148998 | .148998 | 0 | 0 | .375668 | .375668 | .223145 | .223145 | .617913 | .617913 | 1.20392 | 1.20392 |
| 10 | .148624 | .148621 | .688751 | .009524 | .375607 | .375588 | .223136 | .223137 | .617890 | .617905 | 1.20387 | 1.20391 |
| 20 | .147501 | .147494 | 1.37346 | .018996 | .375426 | .375351 | .223109 | .223116 | .617820 | .617883 | 1.20373 | 1.20389 |
| 30 | .145640 | .145625 | 2.05011 | .028364 | .375124 | .374957 | .223064 | .223079 | .617706 | .617846 | 1.20350 | 1.20385 |
| 40 | .135791 | .135734 | 3.99154 | .055323 | .373502 | .372865 | .222830 | .222887 | .617116 | .617649 | 1.20232 | 1.20364 |
| 50 | .120113 | .120001 | 5.71738 | .079478 | .370830 | .369512 | .222461 | .222582 | .616235 | .617335 | 1.20062 | 1.20332 |
| 60 | .099663 | .099497 | 7.12453 | .099453 | .367164 | .365097 | .221990 | .222183 | .615201 | .616926 | 1.19873 | 1.20289 |
| 70 | .075822 | .075619 | 8.11670 | .113912 | .362605 | .359884 | .221459 | .221717 | .614181 | .616450 | 1.19700 | 1.20240 |
| 80 | .050208 | .049995 | 8.60876 | .121597 | .357312 | .354205 | .220916 | .221216 | .613344 | .615938 | 1.19577 | 1.20187 |

**Table 6**
Dimensionless frequencies for rotating beam with different inclination angle ($\eta=1000$, $\overline{R}=1$, $k=.003$).

| $\alpha$ (deg.) | $\varepsilon_c^{\max}$ ($10^{-5}$) | | $\varepsilon_b^{\max}$ ($10^{-3}$) | $v_{tip}/L_T$ | $K_1$ ($10^{-2}$) | | $K_2$ ($10^{-1}$) | | $K_3$ ($10^{-1}$) | | $K_4$ | |
|---|---|---|---|---|---|---|---|---|---|---|---|---|
| | EA | EC | EA | EA | EA | EC | EA | EC | EA | EC | EA | EC |
| 0 | 1.34094 | 1.34094 | 0 | 0 | .529054 | .529054 | .247469 | .247469 | .646623 | .646623 | .124064 | .124064 |
| 10 | 1.33742 | 1.33755 | .401966 | .042755 | .528948 | .528552 | .247408 | .247410 | .646343 | .646557 | .124020 | .124057 |
| 20 | 1.32688 | 1.32740 | .802883 | .085366 | .528626 | .527049 | .247224 | .247232 | .645506 | .646361 | .123887 | .124036 |
| 30 | 1.30939 | 1.31058 | 1.20170 | .127689 | .528088 | .524546 | .246917 | .246936 | .644121 | .646036 | .123670 | .124001 |
| 40 | 1.21666 | 1.22157 | 2.37507 | .251535 | .525149 | .511096 | .245271 | .245364 | .636859 | .644310 | .122559 | .123815 |
| 50 | 1.06851 | 1.07997 | 3.49175 | .367905 | .520114 | .488923 | .242565 | .242842 | .625541 | .641553 | .120920 | .123519 |
| 60 | .874165 | .895442 | 4.52322 | .473573 | .512761 | .458389 | .238860 | .239513 | .611240 | .637939 | .118999 | .123132 |
| 70 | .645893 | .680549 | 5.44045 | .565891 | .502734 | .419991 | .234253 | .235572 | .595231 | .633700 | .117027 | .122679 |
| 80 | .398360 | .449942 | 6.21305 | .642909 | .489484 | .374358 | .228875 | .231264 | .578803 | .629113 | .115176 | .122190 |

## 3. Numerical examples

To verify the accuracy of the present method and to investigate the steady deformation and the natural frequencies of rotating inclined beams with different inclination angle $\alpha$, dimensionless radius of the hub $\overline{R}$, and slenderness ratios $\eta$ at different dimensionless angular velocities $k$, several dimensionless numerical examples are studied here.

For simplicity, only the uniform beam with rectangular cross section is considered here. The maximum steady state axial strain $\varepsilon_{\max}$ of rotating beam is the sum of the maximum steady state membrane strain $\varepsilon_c^{\max}$ and bending strain $\varepsilon_b^{\max}$, which occur at the root of the rotating beam. In practice, rotating structures are designed to operate in the elastic range of the materials. Thus, it is considered that $\varepsilon_{\max} \le \varepsilon_y$ (say .01) in this study. At the same dimensionless angular speed $k$, $\varepsilon_{\max}$ are different for rotating

**Table 7**
Dimensionless frequencies for rotating beam with different slenderness ratio ($\overline{R}=0$).

| $\eta$ | $k$ | $\varepsilon_c^{\max}$ ($10^{-4}$) | $K_1$ | $K_2$ | $K_3$ | $K_4$ | $K_5$ | $K_6$ | $K_7$ |
|---|---|---|---|---|---|---|---|---|---|
| 20 | 0 | 0 | .174787 | 1.05953 | 1.57086 ($a$) | 2.82431 | 4.71413 ($a$) | 5.19120 | 7.86206 ($a$) |
| | .01 | .499954 | .174823 | 1.05972 | 1.57096 ($a$) | 2.82446 | 4.71417 ($a$) | 5.19127 | 7.86208 ($a$) |
| | .02 | 2.00007 | .174930 | 1.06027 | 1.57127 ($a$) | 2.82489 | 4.71427 ($a$) | 5.19148 | 7.86213 ($a$) |
| | .04 | 8.00427 | .175354 | 1.06248 | 1.57251 ($a$) | 2.82663 | 4.71467 ($a$) | 5.19234 | 7.86236 ($a$) |
| | .06 | 18.0246 | .176054 | 1.06615 | 1.57458 ($a$) | 2.82952 | 4.71533 ($a$) | 5.19377 | 7.86273 ($a$) |
| 50 | 0 | 0 | .0702550 | .437859 | 1.21530 | 1.57086 ($a$) | 2.35176 | 3.82646 | 4.71413 ($a$) |
| | .01 | .499954 | .0703844 | .438455 | 1.21592 | 1.57096 ($a$) | 2.35238 | 3.82704 | 4.71417 ($a$) |
| | .02 | 2.00007 | .0707689 | .440240 | 1.21780 | 1.57125 ($a$) | 2.35425 | 3.82879 | 4.71426 ($a$) |
| | .04 | 8.00427 | .0722524 | .447313 | 1.22528 | 1.57240 ($a$) | 2.36171 | 3.83581 | 4.71466 ($a$) |
| | .06 | 18.0246 | .0745530 | .458872 | 1.23765 | 1.57433 ($a$) | 2.37409 | 3.84748 | 4.71531 ($a$) |
| 100 | 0 | 0 | .0351520 | .219989 | .614602 | 1.20047 | 1.57086 ($a$) | 1.97619 | 2.93707 |
| | .01 | .499954 | .0354205 | .221216 | .615938 | 1.20187 | 1.57096 ($a$) | 1.97760 | 2.93847 |
| | .02 | 2.00007 | .0361954 | .224860 | .619929 | 1.20605 | 1.57124 ($a$) | 1.98183 | 2.94267 |
| | .04 | 8.00427 | .0389181 | .238890 | .635620 | 1.22261 | 1.57239 ($a$) | 1.99865 | 2.95942 |
| | .06 | 18.0246 | .0425305 | .260607 | .660876 | 1.24968 | 1.57431 ($a$) | 2.02636 | 2.98715 |
| 500 | 0 | 0 | .00703197 | .0440661 | .123375 | .241735 | .399539 | .596720 | .833235 |
| | .01 | .499954 | .00814757 | .0498972 | .130004 | .248856 | .406927 | .604274 | .840899 |
| | .02 | 2.00007 | .0100978 | .0642386 | .147927 | .268932 | .428225 | .626321 | .863435 |
| | .04 | 8.00427 | .0135687 | .102725 | .202962 | .335905 | .503267 | .706764 | .947569 |
| | .06 | 18.0246 | .0164590 | .145081 | .268690 | .421555 | .605093 | .821022 | 1.07120 |
| 1000 | 0 | 0 | .00351601 | .0220341 | .0616949 | .120893 | .199838 | .298509 | .416903 |
| | .01 | .499954 | .00504927 | .0321223 | .0739765 | .134505 | .214203 | .313344 | .432052 |
| | .02 | 2.00007 | .00677821 | .0513635 | .101497 | .168006 | .251762 | .353634 | .474228 |
| | .04 | 8.00427 | .00942143 | .0942683 | .169116 | .257543 | .360229 | .477630 | .610650 |
| | .06 | 18.0246 | .0116029 | .138373 | .240912 | .355544 | .483657 | .624839 | .779391 |

**Table 8**
Dimensionless frequencies for rotating beam with different inclination angle ($\eta$=20, $\overline{R}=1$).

| $\alpha$ (deg.) | $k$ | $\varepsilon_c^{\max}$ ($10^{-4}$) | $\varepsilon_b^{\max}$ ($10^{-3}$) | $v_{tip}/L_T$ ($10^{-3}$) | $K_1$ | $K_2$ | $K_3$ ($a$) | $K_4$ | $K_5$ ($a$) | $K_6$ | $K_7$ ($a$) |
|---|---|---|---|---|---|---|---|---|---|---|---|
| 0 | 0 | 0 | 0 | 0 | .174787 | 1.05953 | 1.57086 | 2.82431 | 4.71413 | 5.19120 | 7.86206 |
| | .01 | 1.48998 | 0 | 0 | .175258 | 1.06004 | 1.57096 | 2.82469 | 4.71417 | 5.19138 | 7.86208 |
| | .02 | 5.96058 | 0 | 0 | .176661 | 1.06156 | 1.57127 | 2.82581 | 4.71427 | 5.19194 | 7.86213 |
| | .04 | 23.8527 | 0 | 0 | .182150 | 1.06762 | 1.57252 | 2.83030 | 4.71467 | 5.19418 | 7.86236 |
| | .06 | 53.7076 | 0 | 0 | .190897 | 1.07766 | 1.57460 | 2.83779 | 4.71533 | 5.19792 | 7.86273 |
| 5 | .005 | .371543 | .0377019 | .108796 | .174905 | 1.05966 | 1.57089 | 2.82441 | 4.71414 | 5.19124 | 7.86206 |
| | .01 | 1.48622 | .150388 | .433403 | .175256 | 1.06004 | 1.57096 | 2.82469 | 4.71417 | 5.19138 | 7.86208 |
| | .02 | 5.94555 | .594973 | 1.70572 | .176655 | 1.06156 | 1.57128 | 2.82581 | 4.71427 | 5.19194 | 7.86213 |
| | .03 | 13.3800 | 1.31504 | 3.73772 | .178959 | 1.06408 | 1.57180 | 2.82768 | 4.71443 | 5.19287 | 7.86222 |
| 15 | .004 | .232994 | .0716798 | .206879 | .174860 | 1.05961 | 1.57088 | 2.82437 | 4.71414 | 5.19122 | 7.86206 |
| | .006 | .524241 | .161163 | .464982 | .174952 | 1.05971 | 1.57090 | 2.82445 | 4.71415 | 5.19126 | 7.86207 |
| | .008 | .931995 | .286224 | .825404 | .175079 | 1.05985 | 1.57093 | 2.82455 | 4.71415 | 5.19131 | 7.86207 |
| | .01 | 1.45627 | .446646 | 1.28723 | .175243 | 1.06003 | 1.57096 | 2.82468 | 4.71417 | 5.19138 | 7.86208 |
| 30 | .004 | .217170 | .138483 | .399691 | .174853 | 1.05961 | 1.57088 | 2.82437 | 4.71414 | 5.19122 | 7.86206 |
| | .006 | .488640 | .311386 | .898436 | .174936 | 1.05970 | 1.57090 | 2.82444 | 4.71415 | 5.19126 | 7.86207 |
| | .008 | .868711 | .553076 | 1.59506 | .175052 | 1.05983 | 1.57093 | 2.82453 | 4.71415 | 5.19130 | 7.86207 |
| | .01 | 1.35740 | .863181 | 2.48796 | .175200 | 1.06000 | 1.57097 | 2.82466 | 4.71416 | 5.19137 | 7.86207 |
| 60 | .004 | .159194 | .239914 | .692486 | .174828 | 1.05959 | 1.57088 | 2.82436 | 4.71414 | 5.19122 | 7.86206 |
| | .006 | .358200 | .539609 | 1.55715 | .174879 | 1.05966 | 1.57090 | 2.82441 | 4.71414 | 5.19124 | 7.86206 |
| | .008 | .636832 | .958813 | 2.76593 | .174950 | 1.05975 | 1.57093 | 2.82448 | 4.71415 | 5.19128 | 7.86207 |
| | .01 | .995114 | 1.49716 | 4.31705 | .175043 | 1.05988 | 1.57097 | 2.82458 | 4.71416 | 5.19133 | 7.86207 |
| 90 | .004 | .0799949 | .277114 | .799932 | .174793 | 1.05956 | 1.57088 | 2.82434 | 4.71414 | 5.19121 | 7.86206 |
| | .006 | .180004 | .623516 | 1.79965 | .174801 | 1.05960 | 1.57090 | 2.82437 | 4.71414 | 5.19122 | 7.86206 |
| | .008 | .320045 | 1.10850 | 3.19889 | .174811 | 1.05965 | 1.57093 | 2.82441 | 4.71415 | 5.19124 | 7.86206 |
| | .01 | .500146 | 1.73208 | 4.99725 | .174826 | 1.05971 | 1.57097 | 2.82446 | 4.71416 | 5.19127 | 7.86206 |

beams with different $\eta$, $\alpha$ and $\overline{R}$. Thus, the allowable $k$ are different for rotating beams with different $\eta$, $\alpha$ and $\overline{R}$ in this study.

To investigate the effect of the consideration of the difference between $v'$ and $\theta$ (see Eq. (17)), and the effect of the lateral deflection on the steady state deformation and the natural frequency of rotating Euler beams, here cases with and without considering the difference between $v'$ and $\theta$, and case without considering the lateral deflection are studied. The corresponding elements are referred to as EA element, EB element and EC element, respectively. For EA element, all terms in Eqs. (56)–(71) are considered; for EB element, the approximations $1+\varepsilon_c \approx 1$ and $1-\varepsilon_c \approx 1$ are used in Eqs. (56)–(71), the term $-(EI\varepsilon_c/L)\int v'_{,xx}\,dx\mathbf{G}_a$ in Eq. (56), the term $-(EI/L)\int v'_{,xx}\,dx$ in Eq. (60), and Eq. (61) are not considered; for EC element, all terms in Eqs. (56)–(71) are considered except the underlined terms in Eq. (59), which are the lateral inertia nodal force corresponding to the steady state deformation induced by the constant rotation.

**Table 9**
Dimensionless frequencies for rotating beam with different inclination angle ($\eta=50$, $\overline{R}=1$).

| $\alpha$ (deg.) | $k$ | $\varepsilon_c^{\max}$ ($10^{-4}$) | $\varepsilon_b^{\max}$ ($10^{-3}$) | $v_{tip}/L_T$ ($10^{-3}$) | $K_1$ ($10^{-1}$) | $K_2$ | $K_3$ | $K_4$ ($a$) | $K_5$ | $K_6$ | $K_7$($a$) |
|---|---|---|---|---|---|---|---|---|---|---|---|
| 0 | 0 | 0 | 0 | 0 | .702550 | .437859 | 1.21530 | 1.57086 | 2.35176 | 3.82646 | 4.71413 |
| | .01 | 1.48998 | 0 | 0 | .714858 | .439405 | 1.21686 | 1.57096 | 2.35330 | 3.82790 | 4.71417 |
| | .02 | 5.96058 | 0 | 0 | .750486 | .444012 | 1.22152 | 1.57125 | 2.35791 | 3.83224 | 4.71426 |
| | .04 | 23.8527 | 0 | 0 | .877636 | .461975 | 1.23999 | 1.57241 | 2.37627 | 3.84954 | 4.71466 |
| | .06 | 53.7076 | 0 | 0 | 1.05339 | .490429 | 1.27012 | 1.57435 | 2.40655 | 3.87823 | 4.71531 |
| 5 | .005 | .371544 | .0937658 | .674872 | .705638 | .438245 | 1.21569 | 1.57089 | 2.35214 | 3.82682 | 4.71414 |
| | .01 | 1.48623 | .368372 | 2.62960 | .714819 | .439402 | 1.21685 | 1.57096 | 2.35330 | 3.82790 | 4.71417 |
| | .02 | 5.94560 | 1.37849 | 9.53161 | .750365 | .443994 | 1.22144 | 1.57134 | 2.35792 | 3.83222 | 4.71428 |
| | .03 | 13.3800 | 2.81927 | 18.5488 | .805930 | .451541 | 1.22898 | 1.57208 | 2.36562 | 3.83940 | 4.71448 |
| 15 | .004 | .232995 | .178621 | 1.28693 | .704475 | .438102 | 1.21554 | 1.57088 | 2.35200 | 3.82668 | 4.71414 |
| | .006 | .524249 | .399999 | 2.87568 | .706875 | .438404 | 1.21584 | 1.57090 | 2.35231 | 3.82696 | 4.71415 |
| | .008 | .932020 | .706460 | 5.06355 | .710224 | .438828 | 1.21626 | 1.57095 | 2.35273 | 3.82736 | 4.71416 |
| | .01 | 1.45632 | 1.09469 | 7.81586 | .714511 | .439370 | 1.21678 | 1.57102 | 2.35328 | 3.82787 | 4.71418 |
| 30 | .004 | .217177 | .345204 | 2.48741 | .704300 | .438086 | 1.21552 | 1.57088 | 2.35199 | 3.82667 | 4.71414 |
| | .006 | .488671 | .773414 | 5.56161 | .706487 | .438369 | 1.21579 | 1.57093 | 2.35228 | 3.82693 | 4.71415 |
| | .008 | .868804 | 1.36686 | 9.80109 | .709550 | .438764 | 1.21615 | 1.57103 | 2.35269 | 3.82730 | 4.71417 |
| | .01 | 1.35761 | 2.11970 | 15.1438 | .713488 | .439268 | 1.21657 | 1.57120 | 2.35322 | 3.82777 | 4.71420 |
| 60 | .004 | .159213 | .598775 | 4.31633 | .703655 | .438030 | 1.21546 | 1.57090 | 2.35194 | 3.82662 | 4.71414 |
| | .006 | .358293 | 1.34391 | 9.67280 | .705054 | .438241 | 1.21562 | 1.57100 | 2.35217 | 3.82681 | 4.71416 |
| | .008 | .637111 | 2.38084 | 17.0989 | .707047 | .438532 | 1.21579 | 1.57124 | 2.35251 | 3.82708 | 4.71420 |
| | .01 | .995750 | 3.70333 | 26.5209 | .709666 | .438899 | 1.21588 | 1.57171 | 2.35298 | 3.82741 | 4.71428 |
| 90 | .004 | .0800204 | .692777 | 4.99678 | .702768 | .437953 | 1.21538 | 1.57090 | 2.35186 | 3.82655 | 4.71414 |
| | .006 | .180129 | 1.55871 | 11.2331 | .703070 | .438068 | 1.21543 | 1.57103 | 2.35201 | 3.82666 | 4.71417 |
| | .008 | .320420 | 2.77081 | 19.9439 | .703545 | .438223 | 1.21541 | 1.57135 | 2.35223 | 3.82680 | 4.71422 |
| | .01 | .501000 | 4.32854 | 31.1046 | .704248 | .438412 | 1.21523 | 1.57200 | 2.35257 | 3.82696 | 4.71432 |

**Table 10**
Dimensionless frequencies for rotating beam with different inclination angle ($\eta=100$, $\overline{R}=1$).

| $\alpha$ (deg.) | $k$ | $\varepsilon_c^{\max}$ ($10^{-4}$) | $\varepsilon_b^{\max}$ ($10^{-3}$) | $v_{tip}/L_T$ ($10^{-3}$) | $K_1$ ($10^{-1}$) | $K_2$ | $K_3$ | $K_4$ | $K_5$($a$) | $K_6$ | $K_7$ |
|---|---|---|---|---|---|---|---|---|---|---|---|
| 0 | 0 | 0 | 0 | 0 | .351520 | .219989 | .614602 | 1.20047 | 1.57086 | 1.97619 | 2.93707 |
| | .01 | 1.48998 | 0 | 0 | .375668 | .223145 | .617913 | 1.20392 | 1.57096 | 1.97967 | 2.94053 |
| | .02 | 5.96058 | 0 | 0 | .439754 | .232350 | .627728 | 1.21418 | 1.57124 | 1.99008 | 2.95089 |
| | .04 | 23.8527 | 0 | 0 | .630513 | .265905 | .665347 | 1.25429 | 1.57240 | 2.03110 | 2.99195 |
| | .06 | 53.7076 | 0 | 0 | .852550 | .313660 | .723130 | 1.31800 | 1.57433 | 2.09747 | 3.05905 |
| 5 | .005 | .371547 | .184151 | 2.62905 | .357700 | .220780 | .615428 | 1.20133 | 1.57089 | 1.97706 | 2.93793 |
| | .01 | 1.48624 | .688752 | 9.52424 | .375607 | .223136 | .617890 | 1.20387 | 1.57105 | 1.97969 | 2.94052 |
| | .02 | 5.94541 | 2.24028 | 27.6708 | .439644 | .232313 | .627575 | 1.21380 | 1.57195 | 1.99029 | 2.95088 |
| | .03 | 13.3786 | 4.02653 | 42.8179 | .528363 | .246845 | .643385 | 1.23009 | 1.57328 | 2.00786 | 2.96808 |
| 15 | .004 | .233001 | .353188 | 5.06288 | .355386 | .220486 | .615117 | 1.20100 | 1.57090 | 1.97674 | 2.93761 |
| | .006 | .524272 | .780114 | 11.0871 | .360170 | .221104 | .615750 | 1.20164 | 1.57102 | 1.97745 | 2.93829 |
| | .008 | .932074 | 1.35273 | 18.9983 | .366779 | .221965 | .616617 | 1.20248 | 1.57128 | 1.97848 | 2.93924 |
| | .01 | 1.45640 | 2.05010 | 28.3642 | .375124 | .223064 | .617706 | 1.20350 | 1.57175 | 1.97983 | 2.94047 |
| 30 | .004 | .217197 | .683351 | 9.79987 | .355048 | .220453 | .615073 | 1.20094 | 1.57097 | 1.97673 | 2.93758 |
| | .006 | .488757 | 1.51201 | 21.5075 | .359457 | .221027 | .615619 | 1.20142 | 1.57136 | 1.97747 | 2.93822 |
| | .008 | .869005 | 2.62751 | 36.9515 | .365619 | .221821 | .616314 | 1.20192 | 1.57227 | 1.97863 | 2.93913 |
| | .01 | 1.35791 | 3.99154 | 55.3226 | .373502 | .222830 | .617116 | 1.20232 | 1.57395 | 1.98028 | 2.94031 |
| 60 | .004 | .159275 | 1.19032 | 17.0972 | .353793 | .220335 | .614922 | 1.20074 | 1.57117 | 1.97666 | 2.93746 |
| | .006 | .358552 | 2.65115 | 37.8356 | .356773 | .220751 | .615186 | 1.20073 | 1.57232 | 1.97748 | 2.93796 |
| | .008 | .637717 | 4.64576 | 65.6798 | .361176 | .221308 | .615331 | 1.20019 | 1.57517 | 1.97899 | 2.93869 |
| | .01 | .996627 | 7.12453 | 99.4533 | .367164 | .221990 | .615201 | 1.19873 | 1.58053 | 1.98153 | 2.93967 |
| 90 | .004 | .0801032 | 1.38534 | 19.9428 | .352036 | .220177 | .614745 | 1.20053 | 1.57127 | 1.97653 | 2.93730 |
| | .006 | .180479 | 3.11508 | 44.6722 | .352910 | .220389 | .614728 | 1.20013 | 1.57288 | 1.97726 | 2.93760 |
| | .008 | .321229 | 5.52865 | 78.8019 | .354544 | .220646 | .614359 | 1.19875 | 1.57704 | 1.97887 | 2.93806 |
| | .01 | .502076 | 8.60877 | 121.597 | .357312 | .220916 | .613344 | 1.19577 | 1.58523 | 1.98193 | 2.93871 |

In this section, $v_{tip}/L_T$ denotes the dimensionless lateral tip deflection of the steady state deformation; $K_i$ denotes the $i$th dimensionless natural frequency of the rotating beam, and denotes that the corresponding vibration mode is lateral vibration at $k=0$; in all tables, the entries with'($a$)' denotes that the corresponding vibration mode is axial vibration at $k=0$.

The example first considered is the rotating inclined beams with dimensionless radius of the hub $\overline{R}=1.5$, inclination angle $\alpha=0^\circ$, $5^\circ$, $30^\circ$, $90^\circ$ and slenderness ratios $\eta=20$, 100, 1000. The present results are shown in Tables 1–3 together with some results available in the literature. In Tables 1–3, EA$n$ and EB$n$, $n=10$, 50 and 100, denote that $n$ equal EA and EB elements,

**Table 11**
Dimensionless frequencies for rotating beam with different inclination angle ($\eta=500$, $\overline{R}=1$).

| $\alpha$ (deg.) | $k$ | $\varepsilon_c^{max}$ ($10^{-5}$) | $\varepsilon_b^{max}$ ($10^{-3}$) | $v_{tip}/L_T$ ($10^{-2}$) | $K_1$ ($10^{-2}$) | $K_2$ ($10^{-1}$) | $K_3$ | $K_4$ | $K_5$ | $K_6$ | $K_7$ |
|---|---|---|---|---|---|---|---|---|---|---|---|
| 0 | 0 | 0 | 0 | 0 | .703197 | .440661 | .123375 | .241735 | .399539 | .596720 | .833235 |
| | .01 | 14.8998 | 0 | 0 | 1.48226 | .578458 | .139137 | .258881 | .417488 | .615179 | .852038 |
| | .02 | 59.6058 | 0 | 0 | 2.65111 | .864577 | .177158 | .303589 | .466489 | .666975 | .905720 |
| | .04 | 238.527 | 0 | 0 | 5.05357 | 1.53227 | .276760 | .432184 | .618642 | .837278 | 1.08978 |
| | .06 | 537.076 | 0 | 0 | 7.46277 | 2.22828 | .385008 | .578158 | .800313 | 1.05084 | 1.33083 |
| 5 | .005 | 3.71523 | .623972 | 3.58503 | .964371 | .478904 | .127486 | .246092 | .404032 | .601297 | .837856 |
| | .01 | 14.8592 | 1.53057 | 5.97156 | 1.48209 | .578323 | .139055 | .258706 | .417215 | .614805 | .851525 |
| | .02 | 59.4466 | 3.35362 | 7.34169 | 2.65094 | .864514 | .177104 | .303407 | .466095 | .666282 | .904574 |
| | .03 | 133.806 | 5.16695 | 7.79682 | 3.84949 | 1.19171 | .224942 | .363905 | .536149 | .743176 | .986233 |
| 15 | .004 | 2.32945 | 1.33657 | 8.25672 | .878114 | .464921 | .125811 | .244238 | .402050 | .599215 | .835658 |
| | .006 | 5.23761 | 2.40353 | 12.7695 | 1.05614 | .493800 | .128805 | .247270 | .405036 | .602116 | .838383 |
| | .008 | 9.30567 | 3.49014 | 15.8100 | 1.26123 | .531886 | .133036 | .251633 | .409363 | .606322 | .842347 |
| | .01 | 14.5349 | 4.57922 | 17.8071 | 1.48067 | .577239 | .138395 | .257330 | .415102 | .611946 | .847700 |
| 30 | .002 | .543143 | .798138 | 5.53097 | .747272 | .446394 | .123905 | .242269 | .400063 | .597231 | .833714 |
| | .004 | 2.16965 | 2.62907 | 16.2583 | .872059 | .462982 | .125115 | .243280 | .400855 | .597815 | .833958 |
| | .006 | 4.86672 | 4.75037 | 25.1546 | 1.05026 | .490506 | .127347 | .245018 | .402093 | .598573 | .834055 |
| | .008 | 8.62862 | 6.91073 | 31.0627 | 1.25602 | .528088 | .131069 | .248188 | .404621 | .600444 | .835114 |
| 60 | .001 | .099571 | .370269 | 2.65157 | .710412 | .441743 | .123473 | .241833 | .399633 | .596811 | .833319 |
| | .002 | .398630 | 1.42467 | 9.94347 | .734584 | .444712 | .123552 | .241842 | .399566 | .596676 | .833067 |
| | .003 | .895261 | 3.00402 | 20.0010 | .779944 | .449239 | .123279 | .241278 | .398722 | .595591 | .831610 |
| | .004 | 1.58240 | 4.90168 | 30.4970 | .846717 | .455709 | .122699 | .240117 | .397048 | .593498 | .828946 |
| 90 | .001 | .050098 | .432814 | 3.11011 | .704972 | .441242 | .123414 | .241769 | .399566 | .596740 | .833244 |
| | .002 | .200817 | 1.72159 | 12.1583 | .714860 | .442553 | .123200 | .241437 | .399113 | .596183 | .832514 |
| | .0025 | .313142 | 2.66832 | 18.5342 | .726241 | .443213 | .122774 | .240833 | .398338 | .595264 | .831370 |
| | .003 | .448275 | 3.79060 | 25.7176 | .743838 | .443815 | .122046 | .239816 | .397053 | .593764 | .829553 |

**Table 12**
Dimensionless frequencies for rotating beam with different inclination angle ($\eta=1000$, $\overline{R}=1$).

| $\alpha$ (deg.) | $k$ | $\varepsilon_c^{max}$ ($10^{-5}$) | $\varepsilon_b^{max}$ ($10^{-3}$) | $v_{tip}/L_T$ ($10^{-2}$) | $K_1$ ($10^{-2}$) | $K_2$($10^{-1}$) | $K_3$($10^{-1}$) | $K_4$ | $K_5$ | $K_6$ | $K_7$ |
|---|---|---|---|---|---|---|---|---|---|---|---|
| 0 | 0 | 0 | 0 | 0 | .351601 | .220341 | .616949 | .120893 | .199838 | .298509 | .416903 |
| | .01 | 14.8998 | 0 | 0 | 1.32579 | .432330 | .885977 | .151847 | .233362 | .333715 | .453260 |
| | .02 | 59.6058 | 0 | 0 | 2.52836 | .766152 | 1.38402 | .216170 | .309504 | .418994 | .545501 |
| | .04 | 238.527 | 0 | 0 | 4.94470 | 1.46591 | 2.47884 | .364608 | .495920 | .640731 | .799060 |
| | .06 | 537.076 | 0 | 0 | 7.35850 | 2.17470 | 3.60269 | .518160 | .691561 | .878499 | 1.07803 |
| 5 | .005 | 3.71469 | .765180 | 5.97101 | .741092 | .289187 | .695390 | .129389 | .208697 | .307592 | .426132 |
| | .01 | 14.8600 | 1.67595 | 7.33957 | 1.32571 | .432299 | .885713 | .151759 | .233177 | .333411 | .452825 |
| | .02 | 59.4715 | 3.47188 | 8.02091 | 2.52828 | .766140 | 1.38394 | .216134 | .309404 | .418777 | .545103 |
| | .03 | 133.890 | 5.19998 | 8.25422 | 3.73627 | 1.11397 | 1.92494 | .289119 | .400294 | .525712 | .665915 |
| 15 | .004 | 2.32637 | 1.74492 | 15.8089 | .630646 | .265964 | .665293 | .125858 | .204796 | .303429 | .421755 |
| | .006 | 5.23165 | 2.83438 | 19.1617 | .854092 | .314085 | .723732 | .132190 | .211269 | .309887 | .428128 |
| | .008 | 9.30220 | 3.92558 | 20.8459 | 1.08760 | .370658 | .798239 | .140759 | .220369 | .319173 | .437418 |
| | .01 | 14.5421 | 5.01583 | 21.8450 | 1.32503 | .432039 | .883572 | .151045 | .231702 | .331041 | .449500 |
| 30 | .002 | .542410 | 1.31451 | 16.2579 | .436038 | .231505 | .625672 | .121676 | .200527 | .299137 | .417464 |
| | .004 | 2.15709 | 3.45508 | 31.0607 | .628041 | .264065 | .655495 | .124158 | .202506 | .300707 | .418660 |
| | .006 | 4.84207 | 5.61912 | 37.4732 | .851749 | .312451 | .712882 | .129769 | .207592 | .305203 | .422605 |
| | .008 | 8.61283 | 7.78577 | 40.6.544 | 1.08529 | .369462 | .788909 | .138171 | .215887 | .312999 | .429813 |
| 60 | .001 | .099657 | .712333 | 9.94341 | .367296 | .222367 | .617842 | .120950 | .199862 | .298514 | .416886 |
| | .002 | .395596 | 2.45079 | 30.4964 | .423367 | .227869 | .613626 | .120111 | .198677 | .297113 | .415275 |
| | .003 | .874165 | 4.52322 | 47.3573 | .512761 | .238860 | .611240 | .118999 | .196928 | .294949 | .412763 |
| | .004 | 1.52872 | 6.63384 | 57.8448 | .617231 | .256517 | .620640 | .118883 | .196085 | .293610 | .411048 |
| 90 | .001 | .050204 | .860795 | 12.1582 | .357433 | .221288 | .616084 | .120749 | .199640 | .298279 | .416639 |
| | .002 | .194123 | 3.21654 | 40.7207 | .400094 | .222722 | .599363 | .118425 | .196788 | .295121 | .413183 |
| | .0025 | .290777 | 4.68882 | 54.0274 | .440751 | .224722 | .587409 | .116668 | .194632 | .292733 | .410601 |
| | .003 | .398359 | 6.21305 | 64.2909 | .489484 | .228875 | .578803 | .115176 | .192739 | .290593 | .408272 |

respectively, are used for discretization, and LAS denotes the linear analytical solution of the steady state deformation given in the Appendix A of this study. For $k=0$, the results of EA and EB are identical; thus only the results of EA are given. It can be seen that for higher natural frequencies of lateral vibration, the discrepancy between the present results and the analytical solutions given in Ref. [31], in which the rotary inertia is not considered, increases with decrease of the slenderness ratio. It seems that the effect of the rotary inertia on the higher natural frequencies of the Euler beam is not negligible when the slenderness ratio is small. It can

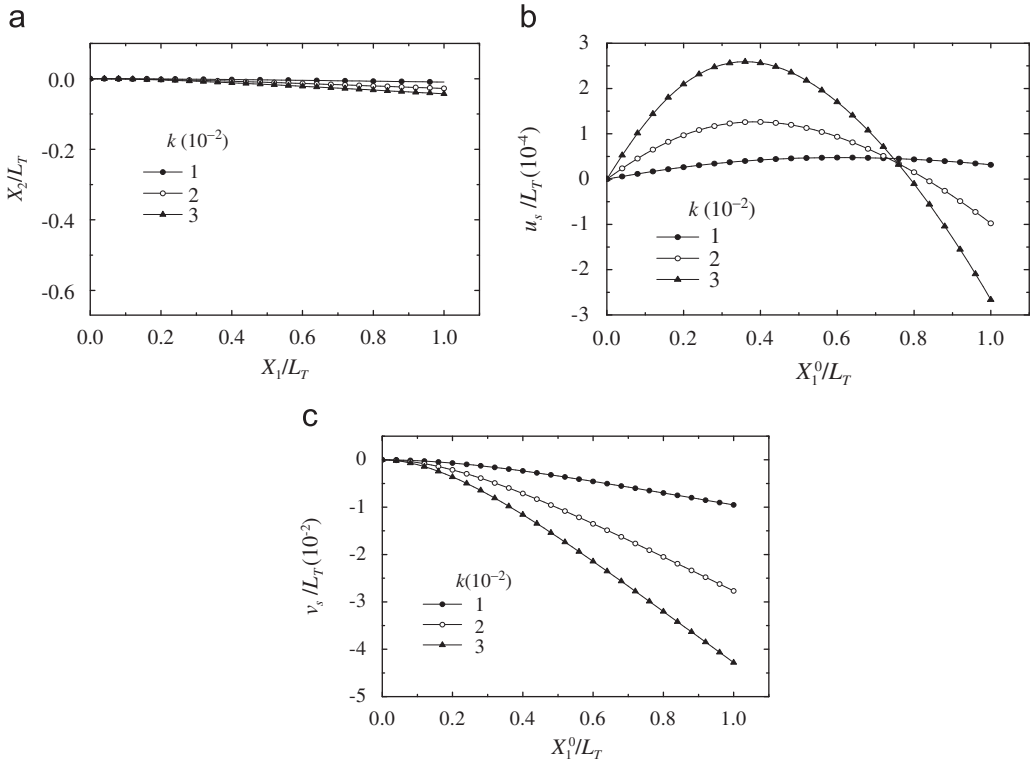


**Fig. 4.** The steady state deformation of rotating beam, (a) deformed configuration, (b) axial displacement and (c) lateral displacement ($\eta=100$, $\overline{R}=1$, $\alpha=5^\circ$).

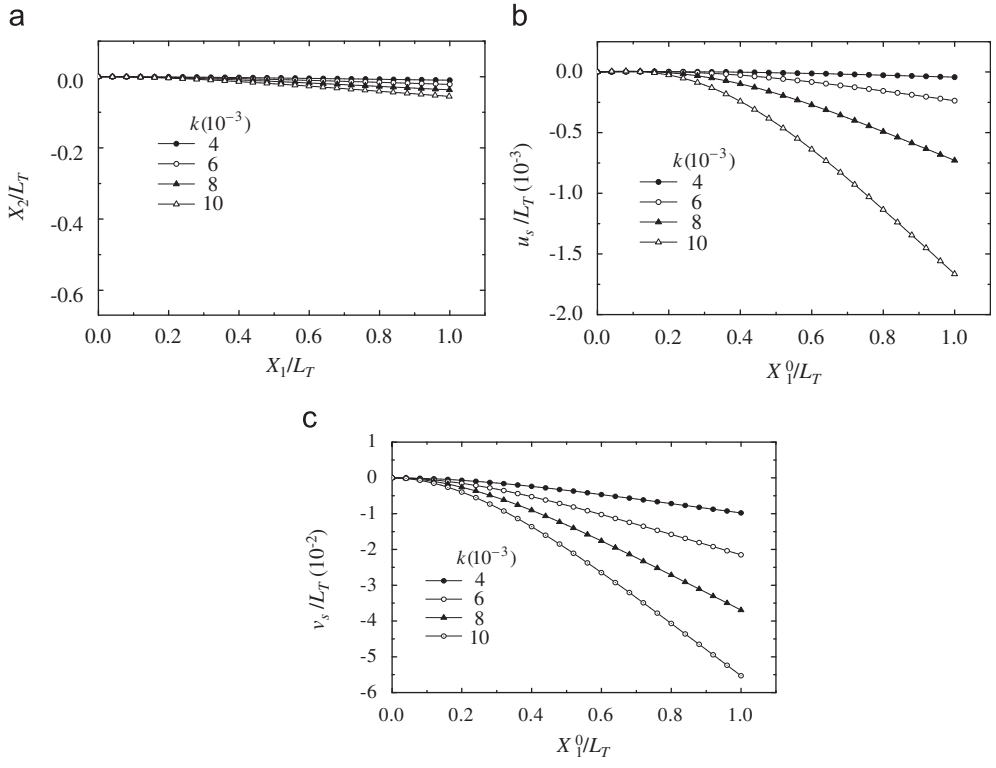


**Fig. 5.** The steady state deformation of rotating beam, (a) deformed configuration, (b) axial displacement and (c) lateral displacement ($\eta=100$, $\overline{R}=1$, $\alpha=30^\circ$).

be seen from Tables 1–3 that the difference between the results of EA and EB is not significant, but still distinguishable. The difference between results of EA50 and EA100 is negligible for all cases studied. Thus, in the rest of the section, all numerical results are obtained using 50 equal EA elements. For $\alpha=0$, and $k\neq 0$, the steady state deformation is axial deformation only as expected. The analytical solution of the maximum steady state membrane strain $\varepsilon_c^{\max}$ given in Ref. [14] and the linear solution given in the Appendix (Eq. (A7)) are identical. It can be seen that at the same dimensionless angular speed $k$, $\varepsilon_c^{\max}$ is independent of the

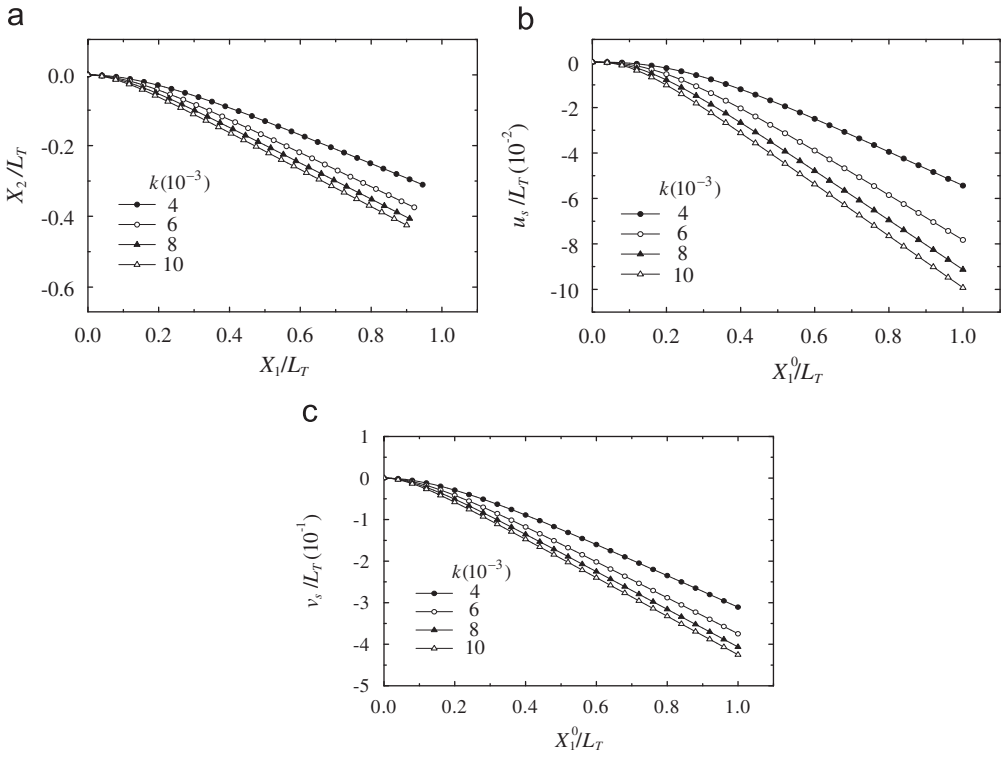


**Fig. 6.** The steady state deformation of rotating beam, (a) deformed configuration, (b) axial displacement and (c) lateral displacement ($\eta=1000$, $\bar{R}=1$, $\alpha=30^\circ$).

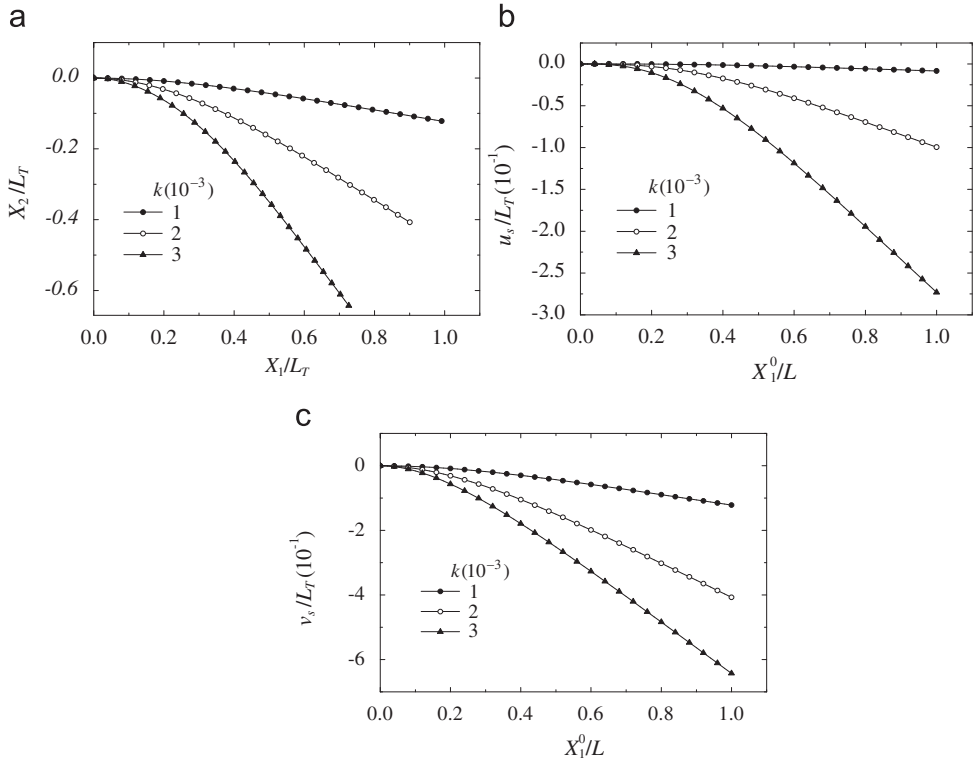


**Fig. 7.** The steady state deformation of rotating beam, (a) deformed configuration, (b) axial displacement and (c) lateral displacement ($\eta=1000$, $\bar{R}=1$, $\alpha=90^\circ$).

slenderness ratio $\eta$. Thus, for $\alpha=0$, the allowable $k$ is limited by $\varepsilon_c^{\max}$, and is the same for the rotating beam with different slenderness ratio $\eta$. Very good agreement is observed between the natural frequencies obtained by the present study and those given in Ref. [23], which are obtained using the power series method. The difference between $v'$ and $\theta$ is not considered in Ref. [23]. It can be seen from Tables 1–3 that with increase of the slenderness ratio $\eta$ and the inclination angle $\alpha$, the values of $\varepsilon_b^{\max}$ and $v_{tip}/L_T$ increase significantly, and the value of the allowable dimensionless angular speed $k$ decrease significantly. The results of EA and LAS have the same tendency. However, the values of the results of EA are smaller than those of LAS.

To investigate the effect of the lateral deflection on the steady state deformation and the natural frequency of rotating inclined beams, the cases (1) $\eta=70$, $\overline{R}=1$, $k=5/70$, (2) $\eta=100$, $\overline{R}=1$, $k=.01$ and (3) $\eta=1000$, $\overline{R}=1$, $k=.003$ are studied with and without considering the lateral deflection. The present results are shown in Tables 4–6. The results transcribed from the Figure given in Ref. [20], in which the steady state lateral deflection and the rotary inertia are not considered, are also shown in Table 4 for comparison. It can be seen from Table 4 that except $\alpha=0$, the values of $\varepsilon_b^{\max}$ are much larger than the yield strain for most engineering materials at $k=5/70$. Thus the results in Table 4 are only displayed for the purpose of comparisons between the results of EC and those given in Ref. [20]. There is a very good agreement between the natural frequencies obtained using the EC element and those given in Ref. [20]. Although the comparisons are beyond the yield point of most engineering materials, results of EA and EC show that the differences between the cases with and without considering the lateral deflection become apparent for the rotating inclined beam with large inclination angle $\alpha$ at high dimensionless angular speed. It can be seen from Tables 4–6

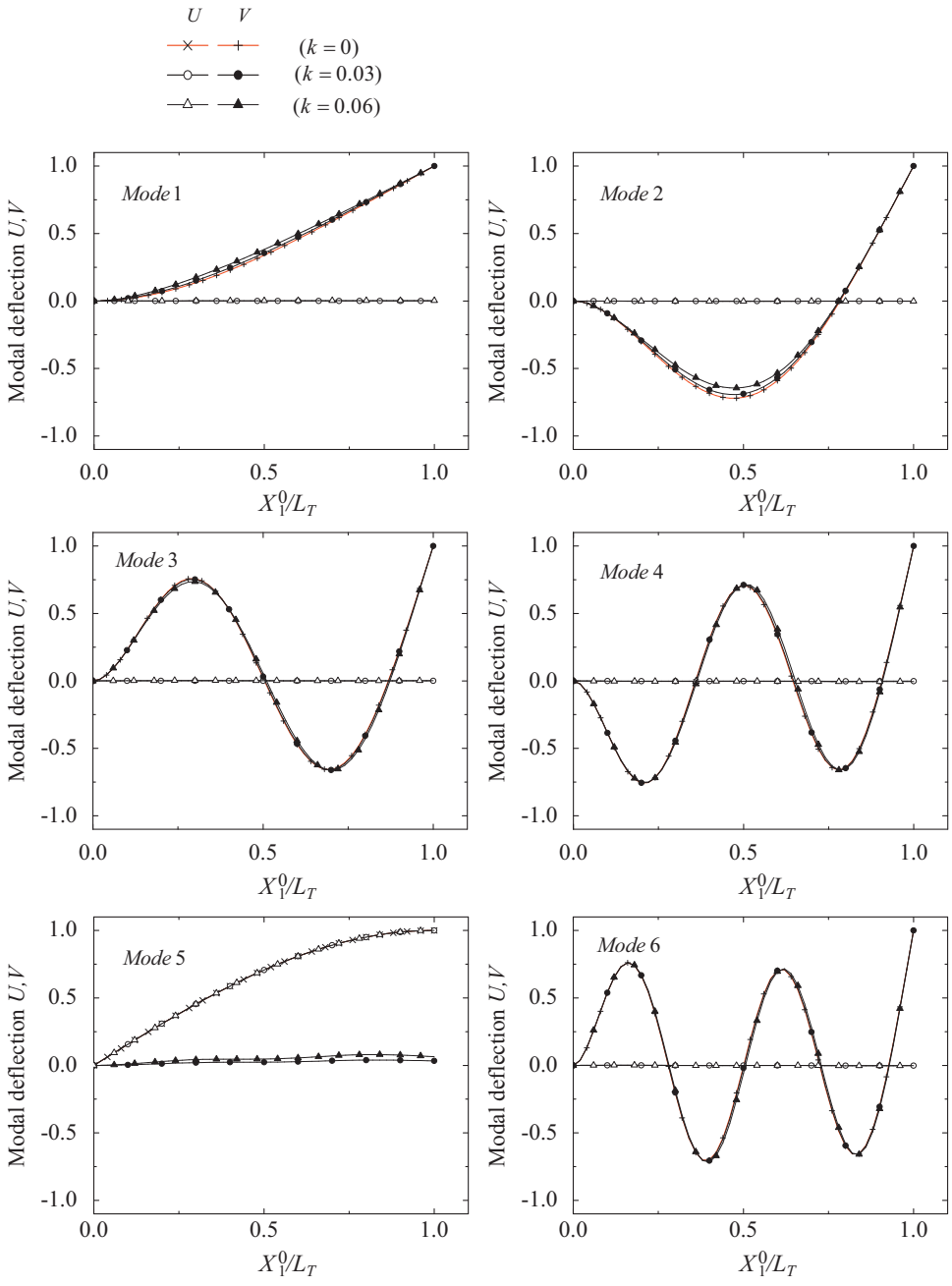


**Fig. 8.** The first six vibration mode shapes of a rotating beam ($\eta=100$, $\overline{R}=1$, $\alpha=0^\circ$).

that both the natural frequencies of EA and EC decrease with increase of $\alpha$. At allowable dimensionless angular speed, the difference between the natural frequencies of EA and EC is not significant for small $\alpha$ or $\eta$, but the first natural frequency of EC is much smaller than that of EA for large $\alpha$ and $\eta=1000$. These may be partially attributed to that the centrifugal stiffening effect of the rotating inclined beam decreases with increase of the inclination angle $\alpha$; but this decrease is alleviated by the steady state lateral deflections, which increase significantly with increase of inclination angle and slenderness ratio $\eta$ of the rotating beam.

To investigate the effect of angular speed on the steady state deformation and natural frequency of rotating beams with different slenderness ratios and inclination angles, the following cases are considered: slenderness ratio $\eta=20$, 50, 100, 500, 1000, inclination angle $\alpha=0^\circ$, $5^\circ$, $15^\circ$, $30^\circ$, $60^\circ$, $90^\circ$ and dimensionless radius of the rotating hub $\overline{R}=0$, 1. Tables 7–12 tabulate the maximum steady state membrane strain and bending strain, dimensionless lateral tip deflection, and first seven dimensionless natural frequencies for different $\eta$. It can be seen from Eqs. (23)–(26) and (59), or Eq. (A5) that the lateral component of the centrifugal force in the rotating inclined beam with $\overline{R}=0$ is zero. Thus, for cases with $\overline{R}=0$, the steady state lateral deflection is zero and the natural frequencies are all the same for the rotating beam with different inclination angle $\alpha$. It can be seen from Tables 8–12 that the values of $v_{tip}/L_T$, which is very small for $\eta=20$ and 50, increase significantly with increase of the dimensionless angular velocities $k$ and slenderness ratio $\eta$. Comparing the results of EA with the results of linear analytical solution given in Eq. (A9), which is proportional to $\eta^2k^2$, it is found that the difference between the results of EA and LAS is insignificant for $\eta=20$ and 50, but is remarked for $\eta=500$ and 1000. These may be explained as follows. The centrifugal stiffening effect is significant for slender beam, and the lateral component of the centrifugal force in the rotating inclined beam decreases with the increase of the steady state lateral deflection. For a rotating inclined beam with different inclination angle $\alpha$, it seems that there is a different threshold of $\eta k$ below which the centrifugal stiffening effect is negligible, and there is a different threshold of steady state lateral deflection below which the decrease of the lateral component of the centrifugal force is negligible. Due to the stiffening effect of the centrifugal force, as expected, it can be seen from Tables 10–12 that the lower natural frequencies of lateral vibration increase remarked with increase of the dimensionless angular speed for slender beam with $\alpha\leq 30^\circ$. It may also be

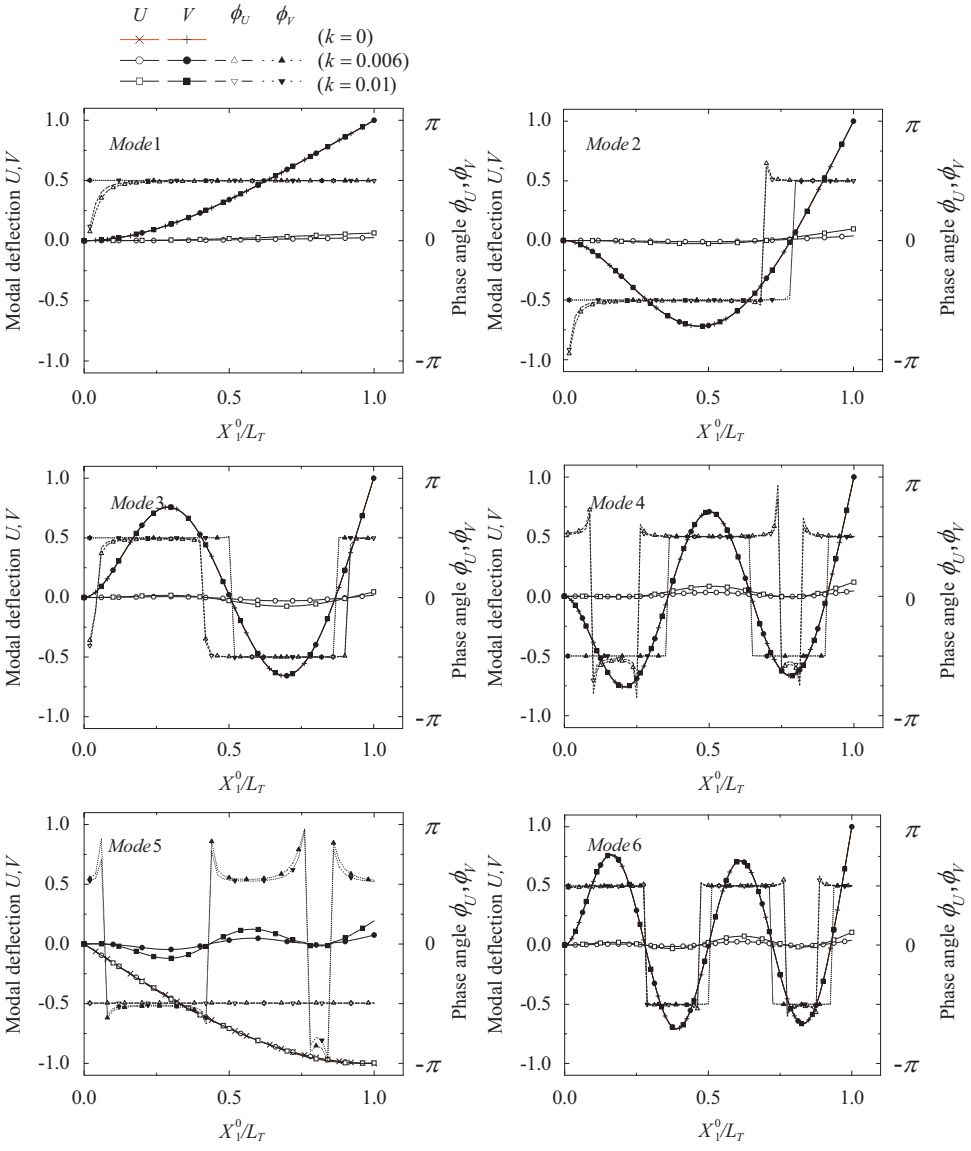


**Fig. 9.** The first six vibration mode shapes of a rotating beam ($\eta=100$, $\overline{R}=1$, $\alpha=30^\circ$).

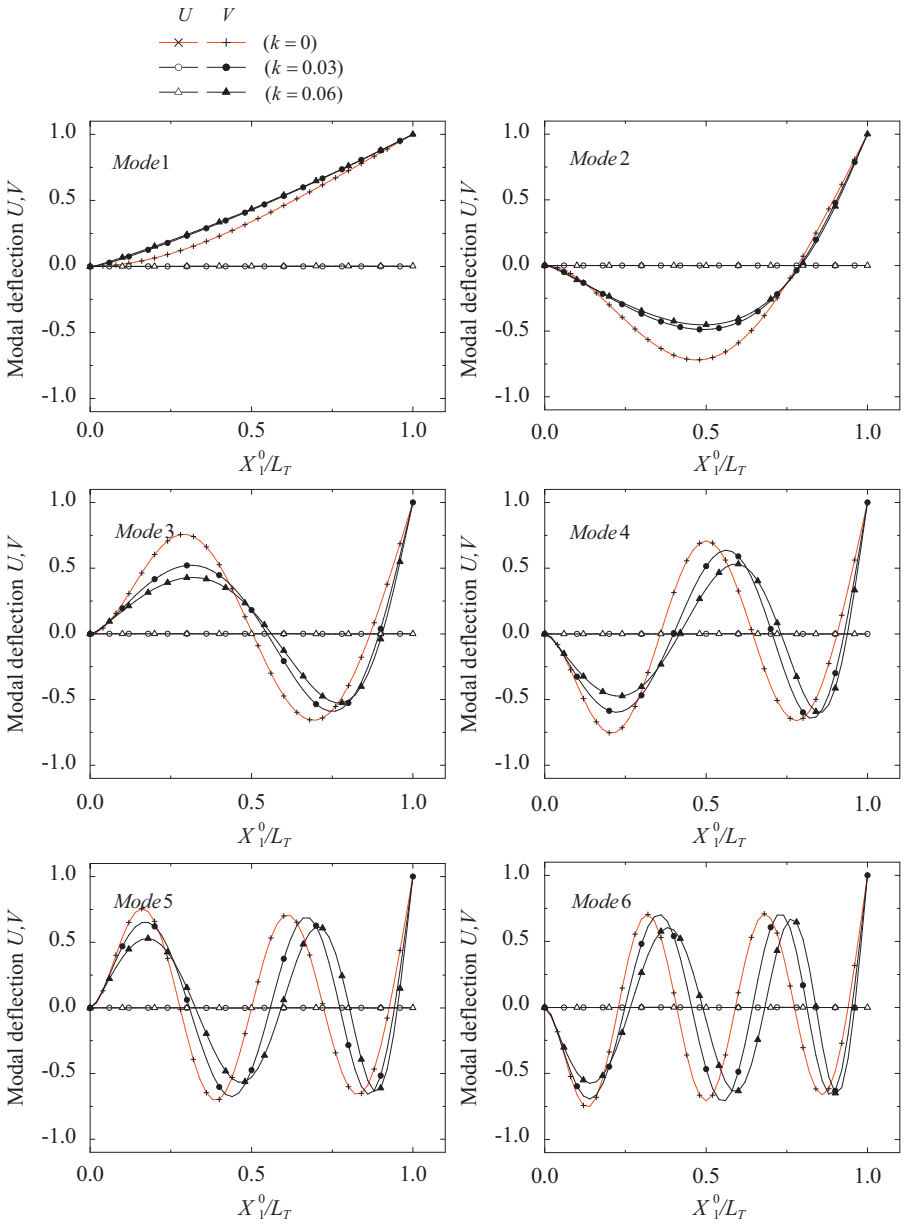


**Fig. 10.** The first six vibration mode shapes of a rotating beam ($\eta=1000$, $\overline{R}=1$, $\alpha=0^\circ$).

noted that the higher natural frequencies of lateral vibration slightly increase first, then slightly decrease with increase of the dimensionless angular speed higher for slender beam with $\alpha \geq 60^\circ$.

Figs. 4–7 show the deformed configurations, axial displacements and lateral displacements for the steady state deformation of rotating beams with $\eta=100$, $\alpha=5^\circ$, $30^\circ$, and $\eta=1000$, $\alpha=30^\circ$, $90^\circ$ at different dimensionless angular speeds. In Figs. 4–7, the $X_1$ and $X_2$ coordinates of the deformed configurations of rotating beam are present at the same scale, and $X_1^0$ denotes the global Lagrangian coordinate of the beam axis.

Figs. 8–11 show the first six vibration modes for rotating beams with slenderness ratio $\eta=100$, 1000, and inclination angle $\alpha=0^\circ$, $30^\circ$ at different dimensionless angular speeds. In Figs. 8–11 $U$ and $V$ denote the $X_1$ and $X_2$ components of the vibration mode, respectively. The definitions of $U$ and $V$ are given by

$$U=(U_R^2+U_I^2)^{1/2}sign(\sin\phi_u),\quad \sin\phi_u=U_I/(U_R^2+U_I^2)^{1/2},$$
$$-\pi\leq\phi_u\leq\pi$$

$$V=(V_R^2+V_I^2)^{1/2}sign(\sin\phi_v),\quad \sin\phi_v=V_I/(V_R^2+V_I^2)^{1/2},$$
$$-\pi\leq\phi_v\leq\pi$$

$$sign(x)=\begin{cases}1 & for\ x>0\\ -1 & for\ x<0\end{cases}$$

where $U_R$ and $V_R$, and $U_I$ and $V_I$ are the $X_1$ and $X_2$ components of $\mathbf{Q}_R$ and $\mathbf{Q}_I$, real part and imaginary part of the vibration mode given in Eq. (78), respectively. $\phi_u$ and $\phi_v$ are phase angles. For non-rotating beam, $\phi_u=\phi_v=0$; for rotating beam ($k\neq 0$) with inclination angle $\alpha=0$, $\phi_u=0$, and $\varphi_v=\pi/2$. Thus, the phase angles for cases with $\alpha=0$ or $k=0$ are not shown in Figs. 8–11. It can be seen from Figs. 8–11, and Tables 10 and 12 that all vibration modes shown in Figs. 8–11 are lateral vibration at $k=0$, except the fifth vibration mode of $\eta=100$. It can be seen from Figs. 8 and 10 that when $\alpha=0$, the difference between the vibration modes of rotating beam at different $k$ is not significant for $\eta=100$, but is very significant for $\eta=1000$. Due to the steady state lateral deformation,

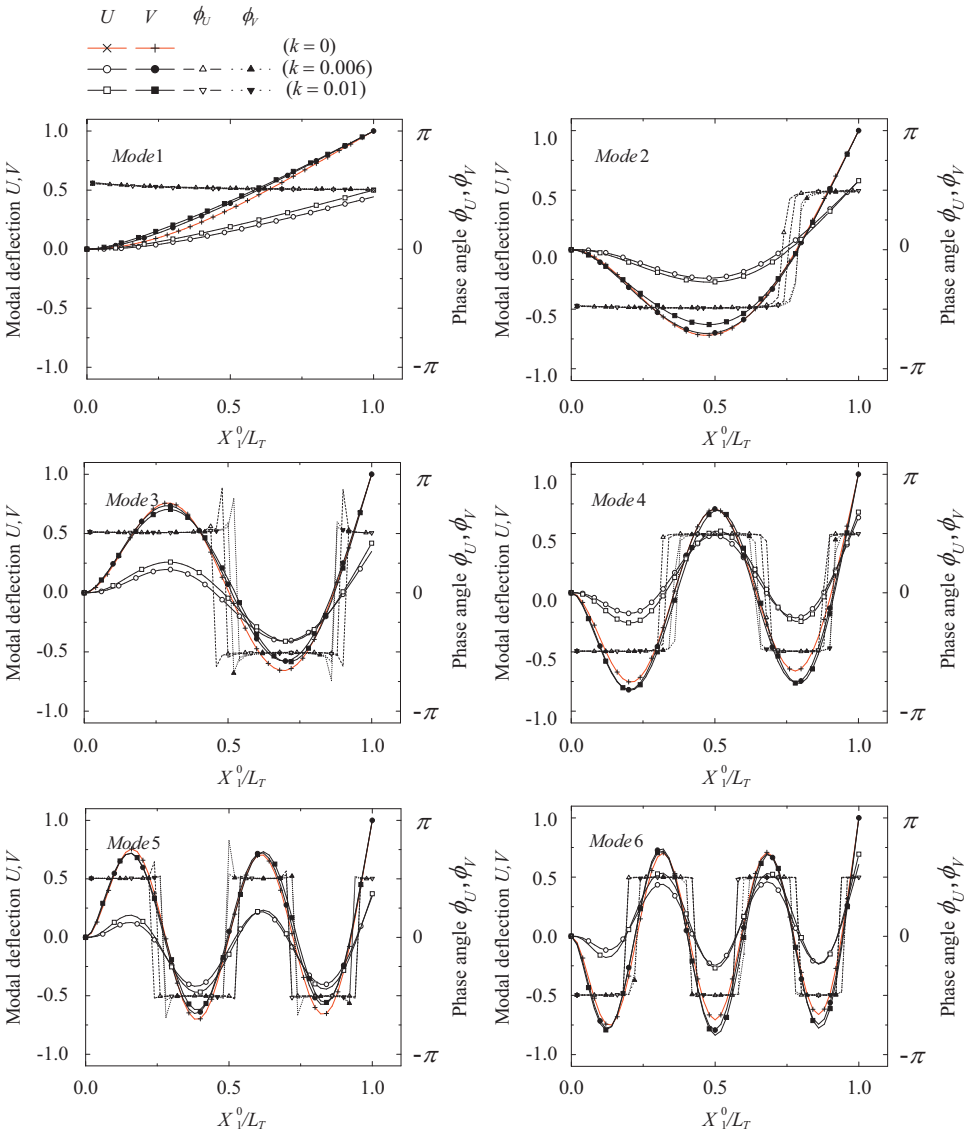


**Fig. 11.** The first six vibration mode shapes of a rotating beam ($\eta=1000$, $\overline{R}=1$, $\alpha=30^\circ$).

it can be seen from Figs. 9 and 11 that when $\alpha=30^\circ$, $k\neq 0$, all vibration modes consist of the $X_1$ and $X_2$ components.

## 4. Conclusions

In this paper, the steady state deformation and the natural frequency of infinitesimal free vibration measured from the position of the corresponding steady state deformation are investigated for rotating the inclined Euler beams with different inclination angles, slenderness ratios and angular speeds of the hub. A corotational finite element formulation combined with the rotating frame method is proposed to derive the equations of motion for a rotating inclined Euler beam with zero setting angle at constant angular velocity. The element deformation and inertia nodal forces are systematically derived by the virtual work principle, the d'Alembert principle, and consistent linearization of the fully geometrically nonlinear beam theory in the current element coordinates. The equations of motion of the system are defined in terms of an inertia global coordinate system, which is coincident with a rotating global coordinate system rigidly tied to the rotating hub, while the total strains in the beam element are measured in an inertia element coordinate system, which is coincident with a rotating element coordinate system constructed at the current configuration of the beam element. The rotating element coordinates rotate about the hub axis at the angular speed of the hub.

The results of dimensionless numerical examples show that the geometrical nonlinearities that arise due to steady state lateral and axial deformations should be considered for the natural frequencies of the inclined rotating beams. The maximum steady state bending strain and lateral deformation increase significantly, but the allowable dimensionless angular speed decreases significantly with increase of inclination angle and slenderness ratio of the rotating beam. It seems that the allowable dimensionless angular speed of the inclined rotating beam is limited by the steady state bending strain, when the inclination angle $\alpha>5^\circ$. Due to the effect of the centrifugal stiffening, the lower dimensionless natural frequencies of lateral vibration increase remarked with increase of the dimensionless angular speed and dimensionless hub radius for slender beam. The centrifugal stiffening effect of the rotating inclined beam decreases with increase of the inclination angle. However, this decrease is alleviated by the steady state lateral deflections, which increase significantly with increase of inclination angle and slenderness

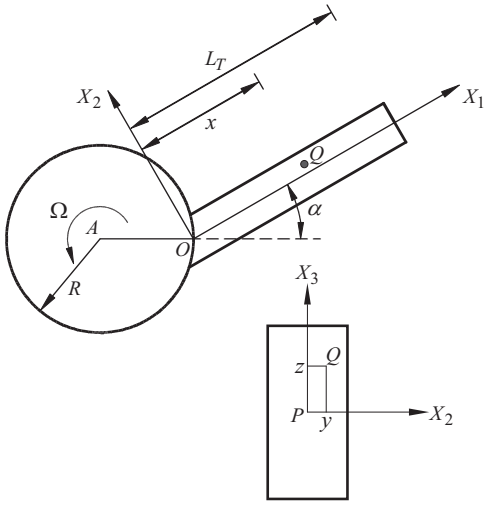


**Fig. A1.** Rotating inclined beam with inclination angle $\alpha$.

ratio of the rotating beam. These may explain why the difference between the first natural frequency of the very slender inclined rotating beam with different inclination angles is not very remarked, but still not negligible.

Finally, it may be emphasized that, although the proposed methods are only applied to the uniform rotating cantilever beams here, the present method can be easily extended to non-uniform rotating beams with discontinuities, as well as with other end conditions.

## Appendix A. Linear steady state deformation of rotating inclined beam

If the tension stiffening effect on bending stiffness and the effect of lateral deflection on the centrifugal force of the rotating inclined beam are not considered, the equivalent distributed load along the beam axis for the rotating inclined beam with rectangular cross section as shown in Fig. A1 may be expressed by

$$\{q_1, q_2, q_3\} = \int_A \mathbf{\Omega} \times (\mathbf{\Omega} \times \mathbf{r}_{AP}) \rho \, dA \tag{A1}$$

$$\mathbf{\Omega} = \{0,0,\Omega\} \tag{A2}$$

$$\mathbf{r}_{AP} = \{R\cos\alpha + x, -R\sin\alpha + y, z\} \tag{A3}$$

where $q_1 = q_1(x)$, $q_2 = q_2(x)$ and $q_3 = q_3(x)$ are the equivalent distributed loads in the $X_1$, $X_2$ and $X_3$ directions, respectively. $\rho$ $A$, and $\Omega$ are density, cross section area and angular speed of the rotating beam, respectively. $\alpha$ is the inclination angle, and $R$ is the radius of the hub. $x$, $y$ and $z$ are the $X_1$, $X_2$ and $X_3$ coordinates of point $Q$, an arbitrary point in the beam.

Substituting Eqs. (A1) and (A2) into Eq. (A3), one may obtain

$$q_1 = \frac{k^2 EA}{L_T^2}(R\cos\alpha + x) \tag{A4}$$

$$q_2 = -\frac{k^2 EA}{L_T^2} R\sin\alpha \tag{A5}$$

$$q_3 = 0 \tag{A6}$$

where $E$ is Young's modulus, $L_T$ is the length of the beam and $k^2 = \rho\Omega^2 L_T^2/E$ is the dimensionless angular speed defined in Eq. (72).

The maximum linear steady state membrane strain induced by $q_1$ occurs at the root of the beam and may be expressed as

$$\varepsilon_{0L}^{\max} = \frac{\int_0^{L_T} q_1 \, dx}{AE} = k^2\left(\overline{R}\cos\alpha + \frac{1}{2}\right) \tag{A7}$$

where $\overline{R} = R/L_T$ is the dimensionless radius of the hub defined in Eq. (72).

For a beam with rectangular cross section of height $h$ and width $b$, the maximum linear steady state bending strain induced by $q_2$ occurs at the top surface of the root of the beam and may be expressed as

$$\varepsilon_{bL}^{\max} = \frac{-q_2 L_T^2}{2EI}\frac{h}{2} = \frac{\sqrt{3}\eta k^2 \overline{R}\sin\alpha}{2} \tag{A8}$$

where $I$ is the moment of inertia of the cross section, $\eta = \sqrt{AL_T^2/I}$ is the slenderness ratio defined in Eq. (72).

The dimensionless linear steady state tip lateral deflection induced by $q_2$ may be expressed by

$$\frac{V_{tip}^L}{L_T} = \frac{-q_y L_T^4}{8EIL_T} = \frac{\eta^2 k^2 \overline{R}\sin\alpha}{8} \tag{A9}$$

## References


[1] Schilhansl MJ. Bending frequency of a rotating cantilever beam. ASME J Appl Mech 1958;25:28–30.
[2] Stafford RO, Giurgiutiu V. Semi-analytic methods for rotating Timoshenko beams. Int J Mech Sci 1975;17:719–27.
[3] Leissa A. Vibrational aspects of rotating turbomachinery blades. ASME Appl Mech Rev 1981;34:629–35.
[4] Hodges DH, Rutkowski MJ. Free-vibration analysis of rotating beams by a variable-order finite-element method. AIAA J 1981;19:1459–66.
[5] Wright AD, Smith CE, Thresher RW, Wang JLC. Vibration modes of centrifugally stiffened beams. ASME J Appl Mech 1982;49:197–202.
[6] Subrahmanyam KB, K.R.V. Kaza. Non-linear flap-lag-extensional vibrations of rotating, pretwisted, preconed beams including Coriolis effects. Int J Mech Sci 1987;29:29–43.
[7] Yokoyama T. Free vibration characteristics of rotating Timoshenko beam. Int J Mech Sci 1988;30:743–55.
[8] Lee SY, Kuo YH. Bending frequency of a rotating beam with an elastically restrained root. ASME J Appl Mech 1991;58:209–14.
[9] Lee HP. Vibration on an inclined rotating cantilever beam with tip mass. ASME J Vib Acoust 1993;115:241–5.
[10] Naguleswaran S. Lateral vibration of a centrifugally tensioned uniform Euler–Bernoulli beam. J Sound Vib 1994;176:613–24.
[11] Crespo Da Silva MRM. A comprehensive analysis of the dynamics of a helicopter rotor blade. Int J Solids Struct 1998;35:619–35.
[12] Yoo HH, Shin SH. Vibration analysis of rotating cantilever beams. J Sound Vib 1998;212:807–28.
[13] Banerjee JR. Dynamic stiffness formulation and free vibration analysis of centrifugally stiffened Timoshenko beams. J Sound Vib 2001;247:97–115.
[14] Lin SC, Hsiao KM. Vibration analysis of rotating Timoshenko beam. J Sound Vib 2001;240:303–22.
[15] Marugabandhu P, Griffin JH. A reduced-order model for evaluating the effect of rotational speed on the natural frequencies and mode shapes of blades. Trans ASME J Eng Gas Turbines Power 2003;125:772–6.
[16] Chandiramani NK, Shete CD, Librescu LI. Vibration of higher-order-shearable pretwisted rotating composite blades. Int J Mech Sci 2003;45:2017–41.
[17] Wang G, Wereley NM. Free vibration analysis of rotating blades with uniform tapers. AIAA J 2004;42:2429–37.
[18] Al-Qaisia AA. Non-linear dynamics of a rotating beam clamped with an attachment angle and carrying an inertia element. Arabian J Sci Eng 2004;29:81–98.
[19] Banerjee JR, Su H. Dynamic stiffness formulation and free vibration analysis of a spinning composite beam. Comput Struct 2006;84:1208–14.
[20] Lee SY, Sheu JJ. Free vibrations of a rotating inclined beam. ASME J Appl Mech 2007;74:406–14.
[21] Lee SY, Sheu JJ. Free vibration of an extensible rotating inclined Timoshenko beam. J Sound Vib 2007;304:606–24.
[22] Gunda JB, Ganguli R. New rational interpolation functions for finite element analysis of rotating beams. Int J Mech Sci 2008;50:578–88.
[23] Huang CL, Lin WY, Hsiao KM. Free vibration analysis of rotating Euler beams at high angular velocity. Comput Struct 2010;88:991–1001.
[24] Khalili SMR, Damanpack AR, Nemati N, Malekzadeh K. Free vibration analysis of sandwich beam carrying sprung masses. Int J Mech Sci 2010;52:1620–33.
[25] Likins PW. Mathematical modeling of spinning elastic bodies for model analysis. AIAA J 1973;11:1251–8.

[26] Simo JC, Vu-Quac K. The role of non-linear theories in transient dynamic analysis of flexible structures. J Sound Vib 1987;119:487–508.
[27] Hsiao KM. Corotational total Lagrangian formulation for three-dimensional beam element. AIAA J 1992;30:797–804.
[28] Hsiao KM, Yang RT, Lee AC. A consistent finite element formulation for nonlinear dynamic analysis of planar beam. Int J Numer Methods Eng 1994;37:75–89.
[29] Chung TJ. Continuum Mechanics. Englewood Cliffs, NJ: Prentice-Hall; 1988.
[30] Malvern DJ. Introduction to the Mechanics of the Continuous Medium. Englewood Cliffs, NJ: Prentice-Hall; 1969.
[31] Rao SS. Mechanical Vibrations. Addison-Wesley; 1986.